

RPA(D) and HRP(A)(D): Two New Models for Calculations of NMR Indirect Nuclear Spin–Spin Coupling Constants

Anna Kristina Schnack-Petersen,^[a] Pi A. B. Haase,^[b] Rasmus Faber,^[c]
Patricio F. Provasi,^[d] and Stephan P. A. Sauer^[e]

In this article, the RPA(D) and HRP(A)(D) models for the calculation of linear response functions are presented. The performance of the new RPA(D) and HRP(A)(D) models is compared to the performance of the established RPA, HRP(A), and SOPPA models in calculations of indirect nuclear spin–spin coupling constants using the CCSD model as a reference. The doubles correction offers a significant improvement on both the RPA and HRP(A) models; however, the improvement is more dramatic in the case of the RPA model. For all coupling types investigated in this study, the

results obtained using the HRP(A)(D) model are comparable in accuracy to those given by the SOPPA model, while requiring between 30% and 90% of the calculation time needed for SOPPA. The RPA(D) model, while of slightly lower accuracy compared to the CCSD model than HRP(A)(D), offered calculation times of only approximately 25% of those required for SOPPA for all the investigated molecules. © 2018 Wiley Periodicals, Inc.

DOI:10.1002/jcc.25712

Introduction

Nuclear magnetic resonance (NMR) spectroscopy is probably the most important experimental technique for identification and structure determination of both organic and inorganic compounds in solution. Nowadays, measurements of NMR spectra are often accompanied by calculations of chemical shifts and indirect nuclear spin–spin coupling constants, the two parameters determining a solution or gas phase NMR spectrum.^[1–3] In particular, the coupling constants can provide important information on, for example, the stereochemistry of compounds,^[4,5] tautomer equilibria,^[6] nonbonded interactions,^[7,8] or potentially even chiral discrimination.^[9,10]

Many methods are already available for these calculations and for instance the CC3,^[11–14] CCSD,^[15–19] and SOPPA^[20–22] models have generally proven to yield results in good agreement with experiment.^[23] Unfortunately, all three methods are computationally too demanding for larger molecules, that is, molecules with more than 30 atoms or more than 800 basis functions, and thus cheaper alternatives are desired. In particular, the inclusion of contributions from doubly excited determinants dramatically increases the demands on computer resources for larger systems. The SOPPA model for instance differs from the underlying RPA model by both second-order contributions to the single excitation contribution and additional double excitation contributions. While the RPA model,^[24,25] corresponding to a coupled Hartree-Fock calculation, is feasible for larger molecules, it lacks electron correlation which is problematic especially for triplet properties, and one might consequently encounter triplet instabilities.^[12,26–28] As an alternative to Hartree-Fock, one often turns to DFT. DFT, however, suffers from the difficulty in choosing an Exchange-Correlation-functional which is suitable for the given system.^[29] There is thus a need for a method for the calculation of molecular

properties which is cheaper than the SOPPA method yet more reliable than, for example, the RPA method.

One such model already exist; the Higher RPA (HRPA) model^[30] includes the second-order correction to the **A** and **B** matrices of SOPPA, while the contributions of the double excitations found in the SOPPA model are still lacking. The importance of the inclusion of double excitation contributions has previously been acknowledged and lead to the development of several methods such as CIS(D),^[31–33] RPA(D),^[34,35] and HRP(A)(D)^[35] for excitation energy calculations with promising results.^[34–39] The double excitation contribution is in these models treated noniteratively as a correction to the results obtained at the CIS, RPA, or HRP(A) level. The same idea has, in

[a] A. K. Schnack-Petersen

Department of Chemistry, University of Copenhagen, Copenhagen, Denmark

E-mail: hjs191@alumni.ku.dk

[b] P. A. B. Haase

Van Swinderen Institute, University of Groningen, Groningen, The Netherlands

[c] R. Faber

Department of Chemistry, Technical University of Denmark, Kgs. Lyngby, Denmark

[d] P. F. Provasi

Department of Physics–IMIT, Northeastern University–CONICET, Corrientes, Argentina

[e] S. P. A. Sauer

Department of Chemistry, University of Copenhagen, Copenhagen, Denmark

E-mail: sauer@kiku.dk

Contract Grant sponsor: Consejo Nacional de Investigaciones Científicas y Técnicas; Contract Grant number: PI: 15/F002 Res. 1017/15 C.S.; Contract Grant sponsor: The World Academy of Sciences; Visiting Expert Programme; Contract Grant number: 3240301376; Contract Grant sponsor: Danish Center for Scientific Computing (DCSC)

© 2018 Wiley Periodicals, Inc.

fact, also been used for the treatment of triple excitations in the CCSDR(3) method.^[40]

In the present work, this idea will once again be used, but now for the calculation of linear response properties and in particular to the calculation of NMR indirect nuclear spin–spin coupling constants. The equations for the new models will be derived in the section “Theory”. The section “Implementation of the RPA(D) and HRP(A) Models” is devoted to a brief discussion of the implementation of the models and in the section “Computational Details”, the methods used for the calculations of the isotropic nuclear spin–spin coupling constants of 20 different molecules and a total of 32 couplings are presented, while the results obtained using the new models will be compared to results obtained using already existing models in the section “Results and Discussion”. It is expected that the doubles correction substantially improves both the RPA and HRP(A) models, hopefully to an extent that leaves the HRP(A) model comparable to SOPPA in accuracy.

Theory

Indirect nuclear spin–spin coupling constant

Indirect nuclear spin–spin coupling constants are a measure of the change in the magnetic field, which a nucleus experiences due to the presence of other nuclei with spin. The direct through space effect is only seen in solid state NMR experiments, while the indirect effect, where the effect of the other nuclei is mediated by electrons between the nuclei, can always be measured. When computing the indirect nuclear spin–spin coupling constant nonrelativistically, one needs to consider four contributions^[41,42]; the diamagnetic spin-orbit (DSO) contribution, which is a simple ground state expectation value, although it can be reformulated as a linear response function,^[43,44] the paramagnetic spin-orbit (PSO) contribution, the spin-dipolar (SD) contribution and finally the Fermi contact (FC) contribution. The three latter contributions are all linear response properties, but while the PSO contribution involves electron spin-independent operators, both the SD and FC contributions are triplet properties.^[41,42]

The equations used for the calculation of indirect spin–spin coupling constants can be derived either from analytical derivatives or using response theory. The former derivation starts from the second derivative of the energy calculated at a given level of theory or from the first derivative of the magnetic moment both in the presence of fields. From the magnetic moment one could also proceed with response theory.

The derivation via analytical derivatives allows one to treat properties as relaxed and unrelaxed, while response theory in its original formulation leads to unrelaxed properties. Originally, frequency-dependent properties could only be obtained via response theory, but are nowadays also available as analytical derivatives of the so-called quasi-energy.

For spin–spin coupling constants these differences are of less importance, as spin–spin coupling constants are frequency

independent and contain triplet properties, which using a relaxed method would be prone to triplet instabilities.

Derivation of the RPA(D) and HRP(A) models

The models used in this study fall in two categories; the ones, where the entire problem is solved iteratively (i.e., RPA, SOPPA, and HRP(A)), and the ones, where a smaller problem is solved iteratively, before a correction is added using pseudo-perturbation theory^[42] to include the missing contributions from a larger model, in this case the SOPPA model. The latter category is the doubles corrected models; RPA(D) and HRP(A)(D), both of which are derived in this study for linear response properties.

The derivation starts in both cases from the matrix representation of the linear response function^[42,45,46] at the SOPPA level in atomic units.

$$\langle\langle\hat{P}_{\alpha}\hat{O}_{\beta}^{\omega}\rangle\rangle_{\omega}=\mathbf{T}^T(\hat{P}_{\alpha})(\omega\mathbf{S}-\mathbf{E})^{-1}\mathbf{T}(\hat{O}_{\beta}^{\omega}) \quad (1)$$

Here, $\mathbf{T}^T(\hat{P}_{\alpha})$ and $\mathbf{T}(\hat{O}_{\beta}^{\omega})$ are property gradients, that is, vectors which elements are the expectation values over the commutator of a given property operator and an excitation (or deexcitation) operator. Furthermore, \mathbf{E} is the Hessian matrix, \mathbf{S} is the overlap matrix in the space of the excitation and deexcitation operators, and ω is the frequency in atomic units corresponding to the perturbing field.

Evaluating the linear response function for a particular combination of operators, \hat{P}_{α} and \hat{O}_{β}^{ω} , implies calculating the inverse of the matrix $(\omega\mathbf{S}-\mathbf{E})$. This is usually avoided by directly calculating the product of the inverse matrix and the right-hand side property gradient, which is called the solution vector $\mathbf{X}_{\beta}(\omega)$. This can be determined by solving the following inhomogeneous system of linear equations:

$$(\omega\mathbf{S}-\mathbf{E})\mathbf{X}_{\beta}(\omega)=\mathbf{T}(\hat{O}_{\beta}^{\omega}) \quad (2)$$

The solution of these equations, which is approximated by perturbation theory in our RPA(D) and HRP(A)(D) models for linear response functions, are derived in the following.

The idea is hereby to expand the matrices and vectors in eq. 2, in a kind of perturbation series, called pseudo-perturbation theory. Rather than starting from the Hamiltonian as in ordinary perturbation theory, we consider the form of the matrices \mathbf{E} and \mathbf{S} and choose the “full” matrices as the ones known from a larger problem—here SOPPA. These can now be partitioned into contributions of different (pseudo-) order, where the zeroth-order matrices are chosen as those corresponding to a smaller known problem—here RPA and HRP(A), respectively.

RPA(D). As the first step one has to define the perturbation for the pseudo-perturbation theory treatment. For that

purpose, the SOPPA matrices^[34,42,47,48] are partitioned into a zeroth-order contribution as well as a first and second-order correction:

$$\mathbf{E}^{[0]} = \begin{pmatrix} \mathbf{A}^{(0,1)} & \mathbf{B}^{(1)} & 0 & 0 \\ \mathbf{B}^{(1)} & \mathbf{A}^{(0,1)} & 0 & 0 \\ 0 & 0 & \mathbf{D}^{(0)} & 0 \\ 0 & 0 & 0 & \mathbf{D}^{(0)} \end{pmatrix} \quad (3)$$

$$\mathbf{E}^{[1]} = \begin{pmatrix} 0 & 0 & \tilde{\mathbf{C}}^{(1)} & 0 \\ 0 & 0 & 0 & \tilde{\mathbf{C}}^{(1)} \\ \mathbf{C}^{(1)} & 0 & 0 & 0 \\ 0 & \mathbf{C}^{(1)} & 0 & 0 \end{pmatrix} \quad (4)$$

$$\mathbf{E}^{[2]} = \begin{pmatrix} \mathbf{A}^{(2)} & \mathbf{B}^{(2)} & 0 & 0 \\ \mathbf{B}^{(2)} & \mathbf{A}^{(2)} & 0 & 0 \\ 0 & 0 & 0 & 0 \\ 0 & 0 & 0 & 0 \end{pmatrix} \quad (5)$$

$$\mathbf{S}^{[0]} = \begin{pmatrix} \mathbf{1} & 0 & 0 & 0 \\ 0 & -\mathbf{1} & 0 & 0 \\ 0 & 0 & \mathbf{1} & 0 \\ 0 & 0 & 0 & -\mathbf{1} \end{pmatrix} \quad (6)$$

$$\mathbf{S}^{[1]} = \begin{pmatrix} 0 & 0 & 0 & 0 \\ 0 & 0 & 0 & 0 \\ 0 & 0 & 0 & 0 \\ 0 & 0 & 0 & 0 \end{pmatrix} \quad (7)$$

$$\mathbf{S}^{[2]} = \begin{pmatrix} \Sigma^{(2)} & 0 & 0 & 0 \\ 0 & -\Sigma^{(2)} & 0 & 0 \\ 0 & 0 & 0 & 0 \\ 0 & 0 & 0 & 0 \end{pmatrix} \quad (8)$$

$$\mathbf{T}(\hat{O}_\beta^\omega)^{[0]} = \begin{pmatrix} e\mathbf{O}_\beta^{\omega(0)} \\ d\mathbf{O}_\beta^{\omega(0)} \\ 0 \\ 0 \end{pmatrix} \quad (9)$$

$$\mathbf{T}(\hat{O}_\beta^\omega)^{[1]} = \begin{pmatrix} 0 \\ 0 \\ e\mathbf{\Omega}_\beta^{\omega(1)} \\ d\mathbf{\Omega}_\beta^{\omega(1)} \end{pmatrix} \quad (10)$$

$$\mathbf{T}(\hat{O}_\beta^\omega)^{[2]} = \begin{pmatrix} e\mathbf{O}_\beta^{\omega(2)} \\ d\mathbf{O}_\beta^{\omega(2)} \\ 0 \\ 0 \end{pmatrix} \quad (11)$$

Note that, all elements of the matrices and vectors in eqs. 3–11 are matrices or vectors, respectively, themselves. Furthermore, the orders of these elements, indicated in superscripts (n), refer to the order in Møller-Plesset perturbation theory, while the order of the whole vector or matrix, indicated in superscripts [n], refer to the order in the pseudo-perturbation theory defined here.

The elements are defined in the following way, where Φ_0 denotes the wavefunction of the reference state, which is here the ground state of the molecule, i, j, k , and l are occupied orbitals, while a, b, c , and d are virtual orbitals, and q_{ai}^\dagger is the single excitation operator, exciting an electron from orbital i to

orbital a . The corresponding deexcitation operator is denoted q_{ai} .

$$A_{ai,bj}^{(0,1,2)} = \langle \Phi_0^{MP} | [q_{ai}, [\hat{F} + \hat{V}, q_{bj}^\dagger]] | \Phi_0^{MP} \rangle^{(0,1,2)} \quad (12)$$

$$B_{ai,bj}^{(1,2)} = \langle \Phi_0^{MP} | [q_{ai}, [\hat{F} + \hat{V}, q_{bj}]] | \Phi_0^{MP} \rangle^{(1,2)} \quad (13)$$

$$D_{aibj,ckdl}^{(0)} = \langle \Phi_0^{SCF} | [q_{ai}q_{bj}, [\hat{F} + \hat{V}, q_{ck}^\dagger q_{dl}^\dagger]] | \Phi_0^{SCF} \rangle^{(0)} \quad (14)$$

$$C_{aibj,ck}^{(1)} = \langle \Phi_0^{SCF} | [q_{ai}q_{bj}, [\hat{F} + \hat{V}, q_{ck}^\dagger]] | \Phi_0^{SCF} \rangle^{(1)} \quad (15)$$

$$\tilde{C}_{ck,aibj}^{(1)} = \langle \Phi_0^{SCF} | [q_{ck}, [\hat{F} + \hat{V}, q_{ai}^\dagger q_{bj}^\dagger]] | \Phi_0^{SCF} \rangle^{(1)} \quad (16)$$

$$\Sigma_{ai,bj}^{(0,2)} = \langle \Phi_0^{MP} | [q_{ai}, q_{bj}^\dagger] | \Phi_0^{MP} \rangle^{(0,2)} \quad (17)$$

$$e\mathbf{O}_{\beta,ai}^{\omega(0,2)} = \langle \Phi_0^{MP} | [q_{ai}, \hat{O}_\beta^\omega] | \Phi_0^{MP} \rangle^{(0,2)} \quad (18)$$

$$d\mathbf{O}_{\beta,ai}^{\omega(0,2)} = \langle \Phi_0^{MP} | [q_{ai}^\dagger, \hat{O}_\beta^\omega] | \Phi_0^{MP} \rangle^{(0,2)} \quad (19)$$

$$e\mathbf{\Omega}_{\beta,aibj}^{\omega(1)} = \langle \Phi_0^{MP} | [q_{ai}q_{bj}, \hat{O}_\beta^\omega] | \Phi_0^{MP} \rangle^{(1)} \quad (20)$$

$$d\mathbf{\Omega}_{\beta,aibj}^{\omega(1)} = \langle \Phi_0^{MP} | [q_{ai}^\dagger q_{bj}^\dagger, \hat{O}_\beta^\omega] | \Phi_0^{MP} \rangle^{(1)} \quad (21)$$

$$e\mathbf{P}_{\alpha,ai}^{(0,2)} = \langle \Phi_0^{MP} | [\hat{P}_\alpha, q_{ai}^\dagger] | \Phi_0^{MP} \rangle^{(0,2)} \quad (22)$$

$$d\mathbf{P}_{\alpha,ai}^{(0,2)} = \langle \Phi_0^{MP} | [\hat{P}_\alpha, q_{ai}] | \Phi_0^{MP} \rangle^{(0,2)} \quad (23)$$

$$e\mathbf{\Pi}_{\alpha,aibj}^{\omega(1)} = \langle \Phi_0^{MP} | [\hat{P}_\alpha, q_{ai}^\dagger q_{bj}^\dagger] | \Phi_0^{MP} \rangle^{(1)} \quad (24)$$

$$d\mathbf{\Pi}_{\alpha,aibj}^{\omega(1)} = \langle \Phi_0^{MP} | [\hat{P}_\alpha, q_{ai}q_{bj}] | \Phi_0^{MP} \rangle^{(1)} \quad (25)$$

Partitioning also the solution vector $\mathbf{X}_\beta(\omega)$ into zeroth, first, and second-order contributions, and using the partitioning of the other vectors and matrices, eq. 2 can be rewritten as

$$\begin{aligned} & \underbrace{\mathbf{T}(\hat{O}_\beta^\omega)^{[0]}}_{0\text{-order contribution}} + \underbrace{\mathbf{T}(\hat{O}_\beta^\omega)^{[1]}}_{1\text{st-order contribution}} + \underbrace{\mathbf{T}(\hat{O}_\beta^\omega)^{[2]}}_{2\text{nd-order contribution}} \\ &= \underbrace{(\omega\mathbf{S}^{[0]} - \mathbf{E}^{[0]})\mathbf{X}_\beta(\omega)^{[0]}}_{0\text{-order contribution}} \\ &+ \underbrace{(\omega\mathbf{S}^{[0]} - \mathbf{E}^{[0]})\mathbf{X}_\beta(\omega)^{[1]} + (\omega\mathbf{S}^{[1]} - \mathbf{E}^{[1]})\mathbf{X}_\beta(\omega)^{[0]}}_{1\text{st-order contribution}} \\ &+ \underbrace{(\omega\mathbf{S}^{[1]} - \mathbf{E}^{[1]})\mathbf{X}_\beta(\omega)^{[1]}}_{2\text{nd-order contribution}} \\ &+ \underbrace{(\omega\mathbf{S}^{[2]} - \mathbf{E}^{[2]})\mathbf{X}_\beta(\omega)^{[0]} + (\omega\mathbf{S}^{[0]} - \mathbf{E}^{[0]})\mathbf{X}_\beta(\omega)^{[2]} + \dots}_{2\text{nd-order contribution}} \quad (26) \end{aligned}$$

As the full property gradient in this case consists of the sum of the zeroth, first, and second-order contributions, any higher-order contributions to the full property gradient must be zero.

The equation can thus be split up into zeroth, first, and second-order equations, where eqs. 3–11 can be inserted. This yields the following zeroth-order equation:

$$\begin{pmatrix} e\mathbf{O}_\beta^{\omega(0)} \\ d\mathbf{O}_\beta^{\omega(0)} \\ 0 \\ 0 \end{pmatrix} = \begin{pmatrix} \omega\mathbf{1}-\mathbf{A}^{(0,1)} & -\mathbf{B}^{(1)} & 0 & 0 \\ -\mathbf{B}^{(1)} & -\omega\mathbf{1}-\mathbf{A}^{(0,1)} & 0 & 0 \\ 0 & 0 & \omega\mathbf{1}-\mathbf{D}^{(0)} & 0 \\ 0 & 0 & 0 & -\omega\mathbf{1}-\mathbf{D}^{(0)} \end{pmatrix} \times \begin{pmatrix} e\mathbf{X}_\beta^{\omega(0)} \\ d\mathbf{X}_\beta^{\omega(0)} \\ e\mathbf{\Xi}_\beta^{\omega(0)} \\ d\mathbf{\Xi}_\beta^{\omega(0)} \end{pmatrix} \quad (27)$$

Due to the form of the zeroth-order property gradient, the double-excitation part of the solution vector must be equal to zero, that is, $e\mathbf{\Xi}_\beta^{\omega(0)} = 0$ and $d\mathbf{\Xi}_\beta^{\omega(0)} = 0$. Thus eq. 27 can be written more compactly as the inhomogeneous system of equations given in eq. 28.

$$\begin{pmatrix} \omega\mathbf{1}-\mathbf{A}^{(0,1)} & -\mathbf{B}^{(1)} \\ -\mathbf{B}^{(1)} & -\omega\mathbf{1}-\mathbf{A}^{(0,1)} \end{pmatrix} \begin{pmatrix} e\mathbf{X}_\beta^{\omega(0)} \\ d\mathbf{X}_\beta^{\omega(0)} \end{pmatrix} = \begin{pmatrix} e\mathbf{O}_\beta^{\omega(0)} \\ d\mathbf{O}_\beta^{\omega(0)} \end{pmatrix} \quad (28)$$

Notice that, solving eq. 28 corresponds to solving the RPA problem.

Likewise, the first-order equation can be written as:

$$\begin{pmatrix} 0 \\ 0 \\ e\mathbf{\Omega}_\beta^{\omega(1)} \\ d\mathbf{\Omega}_\beta^{\omega(1)} \end{pmatrix} = - \begin{pmatrix} 0 & 0 & \tilde{\mathbf{C}}^{(1)} & 0 \\ 0 & 0 & 0 & \tilde{\mathbf{C}}^{(1)} \\ \mathbf{C}^{(1)} & 0 & 0 & 0 \\ 0 & \mathbf{C}^{(1)} & 0 & 0 \end{pmatrix} \begin{pmatrix} e\mathbf{X}_\beta^{\omega(0)} \\ d\mathbf{X}_\beta^{\omega(0)} \\ 0 \\ 0 \end{pmatrix} + \begin{pmatrix} \omega\mathbf{1}-\mathbf{A}^{(0,1)} & -\mathbf{B}^{(1)} & 0 & 0 \\ -\mathbf{B}^{(1)} & -\omega\mathbf{1}-\mathbf{A}^{(0,1)} & 0 & 0 \\ 0 & 0 & \omega\mathbf{1}-\mathbf{D}^{(0)} & 0 \\ 0 & 0 & 0 & -\omega\mathbf{1}-\mathbf{D}^{(0)} \end{pmatrix} \begin{pmatrix} e\mathbf{X}_\beta^{\omega(1)} \\ d\mathbf{X}_\beta^{\omega(1)} \\ e\mathbf{\Xi}_\beta^{\omega(1)} \\ d\mathbf{\Xi}_\beta^{\omega(1)} \end{pmatrix} \quad (29)$$

Due to the form of the first-order property gradient and the zeroth-order solution vector, the first-order solution vector must have its single-excitation part equal to 0. Thus, eq. 29 can be rewritten compactly as the first-order inhomogeneous system of equations in eq. 30.

$$\begin{pmatrix} \omega\mathbf{1}-\mathbf{D}^{(0)} & 0 \\ 0 & -\omega\mathbf{1}-\mathbf{D}^{(0)} \end{pmatrix} \begin{pmatrix} e\mathbf{\Xi}_\beta^{\omega(1)} \\ d\mathbf{\Xi}_\beta^{\omega(1)} \end{pmatrix} = \begin{pmatrix} e\mathbf{\Omega}_\beta^{\omega(1)} \\ d\mathbf{\Omega}_\beta^{\omega(1)} \end{pmatrix} + \begin{pmatrix} \mathbf{C}^{(1)} & 0 \\ 0 & \mathbf{C}^{(1)} \end{pmatrix} \begin{pmatrix} e\mathbf{X}_\beta^{\omega(0)} \\ d\mathbf{X}_\beta^{\omega(0)} \end{pmatrix} \quad (30)$$

As $\mathbf{D}^{(0)}$ is diagonal, this equation is trivial to solve. Finally, the second-order equation can be written as:

$$\begin{pmatrix} e\mathbf{O}_\beta^{\omega(2)} \\ d\mathbf{O}_\beta^{\omega(2)} \\ 0 \\ 0 \end{pmatrix} = - \begin{pmatrix} 0 & 0 & \tilde{\mathbf{C}}^{(1)} & 0 \\ 0 & 0 & 0 & \tilde{\mathbf{C}}^{(1)} \\ \mathbf{C}^{(1)} & 0 & 0 & 0 \\ 0 & \mathbf{C}^{(1)} & 0 & 0 \end{pmatrix} \begin{pmatrix} 0 \\ 0 \\ e\mathbf{\Xi}_\beta^{\omega(1)} \\ d\mathbf{\Xi}_\beta^{\omega(1)} \end{pmatrix} + \begin{pmatrix} \omega\mathbf{1}-\mathbf{A}^{(0,1)} & -\mathbf{B}^{(1)} & 0 & 0 \\ -\mathbf{B}^{(1)} & -\omega\mathbf{1}-\mathbf{A}^{(0,1)} & 0 & 0 \\ 0 & 0 & \omega\mathbf{1}-\mathbf{D}^{(0)} & 0 \\ 0 & 0 & 0 & -\omega\mathbf{1}-\mathbf{D}^{(0)} \end{pmatrix} \begin{pmatrix} e\mathbf{X}_\beta^{\omega(2)} \\ d\mathbf{X}_\beta^{\omega(2)} \\ e\mathbf{\Xi}_\beta^{\omega(2)} \\ d\mathbf{\Xi}_\beta^{\omega(2)} \end{pmatrix} + \begin{pmatrix} \omega\mathbf{\Sigma}^{(2)}-\mathbf{A}^{(2)} & -\mathbf{B}^{(2)} & 0 & 0 \\ -\mathbf{B}^{(2)} & -\omega\mathbf{\Sigma}^{(2)}-\mathbf{A}^{(2)} & 0 & 0 \\ 0 & 0 & \omega\mathbf{1}-\mathbf{D}^{(0)} & 0 \\ 0 & 0 & 0 & -\omega\mathbf{1}-\mathbf{D}^{(0)} \end{pmatrix} \begin{pmatrix} e\mathbf{X}_\beta^{\omega(0)} \\ d\mathbf{X}_\beta^{\omega(0)} \\ 0 \\ 0 \end{pmatrix} \quad (31)$$

Considering that the second-order solution vector like the zeroth-order one must have its double excitation part equal to 0, allows eq. 31 to be compactly written as an inhomogeneous system of equations in the following way:

$$\begin{pmatrix} \omega\mathbf{1}-\mathbf{A}^{(0,1)} & -\mathbf{B}^{(1)} \\ -\mathbf{B}^{(1)} & -\omega\mathbf{1}-\mathbf{A}^{(0,1)} \end{pmatrix} \begin{pmatrix} e\mathbf{X}_\beta^{\omega(2)} \\ d\mathbf{X}_\beta^{\omega(2)} \end{pmatrix} = \begin{pmatrix} e\mathbf{O}_\beta^{\omega(2)} \\ d\mathbf{O}_\beta^{\omega(2)} \end{pmatrix} + \begin{pmatrix} \tilde{\mathbf{C}}^{(1)} & 0 \\ 0 & \tilde{\mathbf{C}}^{(1)} \end{pmatrix} \begin{pmatrix} e\mathbf{\Xi}_\beta^{\omega(1)} \\ d\mathbf{\Xi}_\beta^{\omega(1)} \end{pmatrix} - \begin{pmatrix} \omega\mathbf{\Sigma}^{(2)}-\mathbf{A}^{(2)} & -\mathbf{B}^{(2)} \\ -\mathbf{B}^{(2)} & -\omega\mathbf{\Sigma}^{(2)}-\mathbf{A}^{(2)} \end{pmatrix} \begin{pmatrix} e\mathbf{X}_\beta^{\omega(0)} \\ d\mathbf{X}_\beta^{\omega(0)} \end{pmatrix} \quad (32)$$

The form of the solution vectors can thus be written:

$$\mathbf{X}_\beta(\omega)^{[0]} = \begin{pmatrix} e\mathbf{X}_\beta^{\omega(0)} \\ d\mathbf{X}_\beta^{\omega(0)} \\ 0 \\ 0 \end{pmatrix} \quad (33)$$

$$\mathbf{X}_\beta(\omega)^{[1]} = \begin{pmatrix} 0 \\ 0 \\ e\mathbf{\Xi}_\beta^{\omega(1)} \\ d\mathbf{\Xi}_\beta^{\omega(1)} \end{pmatrix} \quad (34)$$

$$\mathbf{X}_\beta(\omega)^{[2]} = \begin{pmatrix} e\mathbf{X}_\beta^{\omega(2)} \\ d\mathbf{X}_\beta^{\omega(2)} \\ 0 \\ 0 \end{pmatrix} \quad (35)$$

By inserting the partitioned solution vectors, eqs. 33–35, and the property gradient, eqs. 9–11, in the expression for the linear response function, eq. 1, it is possible to obtain an expression for the full linear response function evaluated through second order in pseudo-perturbation theory.

$$\begin{aligned} \langle\langle \hat{P}_{\alpha i}; \hat{O}_\beta^\omega \rangle\rangle_\omega^{RPA(D)} &= \mathbf{T}^T(\hat{P}_\alpha)^{[0]} \mathbf{X}_\beta(\omega)^{[0]} + \mathbf{T}^T(\hat{P}_\alpha)^{[0]} \mathbf{X}_\beta(\omega)^{[1]} \\ &+ \mathbf{T}^T(\hat{P}_\alpha)^{[1]} \mathbf{X}_\beta(\omega)^{[0]} + \mathbf{T}^T(\hat{P}_\alpha)^{[0]} \mathbf{X}_\beta(\omega)^{[2]} \\ &+ \mathbf{T}^T(\hat{P}_\alpha)^{[1]} \mathbf{X}_\beta(\omega)^{[1]} + \mathbf{T}^T(\hat{P}_\alpha)^{[2]} \mathbf{X}_\beta(\omega)^{[0]} \end{aligned} \quad (36)$$

As the property gradient $\mathbf{T}^T(\hat{P}_\alpha)^{[j]}$ has the same form as property gradient $\mathbf{T}(\hat{O}_\beta)^{[j]}$, given in eqs. 9–11, all first-order contributions to the linear response function will be 0, due to the form of the solution vector contributions eqs. 33–35. The zeroth-order contribution will simply be the RPA linear response function, while the second-order contribution offers a correction. Using that a left-hand side zeroth-order solution vector could be written as eq. 37,

$$\left(\epsilon \mathbf{X}_\alpha^{\omega[0]T} d \mathbf{X}_\alpha^{\omega[0]T} \right) = \left(\epsilon \mathbf{P}_\alpha^{(0)} d \mathbf{P}_\alpha^{(0)} \right) \begin{pmatrix} \omega \mathbf{1} - \mathbf{A}^{(0,1)} & -\mathbf{B}^{(1)} \\ -\mathbf{B}^{(1)} & -\omega \mathbf{1} - \mathbf{A}^{(0,1)} \end{pmatrix}^{-1} \quad (37)$$

the linear response function at the RPA(D) level can be written in the following way, where the expression for the first-order solution vector has also been inserted. For simplicity, the expression has been split up in a single excitation part $\langle\langle \hat{P}_\alpha; \hat{O}_\beta^\omega \rangle\rangle_\omega^{RPA(D),S}$ and a double excitation part $\langle\langle \hat{P}_\alpha; \hat{O}_\beta^\omega \rangle\rangle_\omega^{RPA(D),D}$.

$$\langle\langle \hat{P}_\alpha; \hat{O}_\beta^\omega \rangle\rangle_\omega^{RPA(D)} = \langle\langle \hat{P}_\alpha; \hat{O}_\beta^\omega \rangle\rangle_\omega^{RPA(D),S} + \langle\langle \hat{P}_\alpha; \hat{O}_\beta^\omega \rangle\rangle_\omega^{RPA(D),D} \quad (38)$$

$$\begin{aligned} \langle\langle \hat{P}_\alpha; \hat{O}_\beta^\omega \rangle\rangle_\omega^{RPA(D),S} &= \left(\epsilon \mathbf{P}_\alpha^{(0)} d \mathbf{P}_\alpha^{(0)} \right) \begin{pmatrix} \epsilon \mathbf{X}_\beta^{\omega[0]} \\ d \mathbf{X}_\beta^{\omega[0]} \end{pmatrix} + \left(\epsilon \mathbf{X}_\alpha^{\omega[0]T} d \mathbf{X}_\alpha^{\omega[0]T} \right) \begin{pmatrix} \epsilon \mathbf{O}_\beta^{\omega(2)} \\ d \mathbf{O}_\beta^{\omega(2)} \end{pmatrix} \\ &+ \left(\epsilon \mathbf{X}_\alpha^{\omega[0]T} d \mathbf{X}_\alpha^{\omega[0]T} \right) \begin{pmatrix} \mathbf{A}^{(2)} - \omega \Sigma^{(2)} & \mathbf{B}^{(2)} \\ \mathbf{B}^{(2)} & \omega \Sigma^{(2)} + \mathbf{A}^{(2)} \end{pmatrix} \begin{pmatrix} \epsilon \mathbf{X}_\beta^{\omega[0]} \\ d \mathbf{X}_\beta^{\omega[0]} \end{pmatrix} \\ &+ \left(\epsilon \mathbf{P}_\alpha^{(2)} d \mathbf{P}_\alpha^{(2)} \right) \begin{pmatrix} \epsilon \mathbf{X}_\beta^{\omega[0]} \\ d \mathbf{X}_\beta^{\omega[0]} \end{pmatrix} \end{aligned} \quad (39)$$

$$\begin{aligned} \langle\langle \hat{P}_\alpha; \hat{O}_\beta^\omega \rangle\rangle_\omega^{RPA(D),D} &= - \left(\epsilon \mathbf{X}_\alpha^{\omega[0]T} d \mathbf{X}_\alpha^{\omega[0]T} \right) \begin{pmatrix} \tilde{\mathbf{C}}^{(1)} & 0 \\ 0 & \tilde{\mathbf{C}}^{(1)} \end{pmatrix} \begin{pmatrix} \mathbf{D}^{(0)} - \omega \mathbf{1} & 0 \\ 0 & \mathbf{D}^{(0)} + \omega \mathbf{1} \end{pmatrix}^{-1} \\ &\times \left\{ \begin{pmatrix} \epsilon \mathbf{O}_\beta^{\omega(1)} \\ d \mathbf{O}_\beta^{\omega(1)} \end{pmatrix} + \begin{pmatrix} \mathbf{C}^{(1)} & 0 \\ 0 & \mathbf{C}^{(1)} \end{pmatrix} \begin{pmatrix} \epsilon \mathbf{X}_\beta^{\omega[0]} \\ d \mathbf{X}_\beta^{\omega[0]} \end{pmatrix} \right\} \\ &- \left(\epsilon \mathbf{P}_\alpha^{(1)} d \mathbf{P}_\alpha^{(1)} \right) \begin{pmatrix} \mathbf{D}^{(0)} - \omega \mathbf{1} & 0 \\ 0 & \mathbf{D}^{(0)} + \omega \mathbf{1} \end{pmatrix}^{-1} \\ &\times \left\{ \begin{pmatrix} \epsilon \mathbf{O}_\beta^{\omega(1)} \\ d \mathbf{O}_\beta^{\omega(1)} \end{pmatrix} + \begin{pmatrix} \mathbf{C}^{(1)} & 0 \\ 0 & \mathbf{C}^{(1)} \end{pmatrix} \begin{pmatrix} \epsilon \mathbf{X}_\beta^{\omega[0]} \\ d \mathbf{X}_\beta^{\omega[0]} \end{pmatrix} \right\} \end{aligned} \quad (40)$$

We can thus calculate the polarization propagator at the RPA(D) level by only calculating the small RPA problem iteratively.

HRPA(D). The derivation of the HRPA(D) model for linear response properties is completely analogous to the derivation of the RPA(D) model. First, the SOPPA matrices^[42,47,48] are partitioned into a zeroth-order contribution and a first-order correction consisting of the remaining contributions. The zeroth-order contribution differs from the zeroth-order contribution in the derivation of the RPA(D) model, in that it includes also the $\mathbf{A}^{(2)}$, $\mathbf{B}^{(2)}$, and $\Sigma^{(2)}$ matrices and the second-order contributions to the single-excitation part of the property gradients.

$$\mathbf{E}^{[0]} = \begin{pmatrix} \mathbf{A}^{(0,1,2)} & \mathbf{B}^{(1,2)} & 0 & 0 \\ \mathbf{B}^{(1,2)} & \mathbf{A}^{(0,1,2)} & 0 & 0 \\ 0 & 0 & \mathbf{D}^{(0)} & 0 \\ 0 & 0 & 0 & \mathbf{D}^{(0)} \end{pmatrix} \quad (41)$$

$$\mathbf{E}^{[1]} = \begin{pmatrix} 0 & 0 & \tilde{\mathbf{C}}^{(1)} & 0 \\ 0 & 0 & 0 & \tilde{\mathbf{C}}^{(1)} \\ \mathbf{C}^{(1)} & 0 & 0 & 0 \\ 0 & \mathbf{C}^{(1)} & 0 & 0 \end{pmatrix} \quad (42)$$

$$\mathbf{S}^{[0]} = \begin{pmatrix} \mathbf{1} + \Sigma^{(2)} & 0 & 0 & 0 \\ 0 & -\mathbf{1} - \Sigma^{(2)} & 0 & 0 \\ 0 & 0 & \mathbf{1} & 0 \\ 0 & 0 & 0 & -\mathbf{1} \end{pmatrix} \quad (43)$$

$$\mathbf{S}^{[1]} = \begin{pmatrix} 0 & 0 & 0 & 0 \\ 0 & 0 & 0 & 0 \\ 0 & 0 & 0 & 0 \\ 0 & 0 & 0 & 0 \end{pmatrix} \quad (44)$$

$$\mathbf{T}(\hat{O}_\beta)^{[0]} = \begin{pmatrix} \epsilon \mathbf{O}_\beta^{\omega(0,2)} \\ d \mathbf{O}_\beta^{\omega(0,2)} \\ 0 \\ 0 \end{pmatrix} \quad (45)$$

$$\mathbf{T}(\hat{O}_\beta)^{[1]} = \begin{pmatrix} 0 \\ 0 \\ \epsilon \mathbf{O}_\beta^{\omega(1)} \\ d \mathbf{O}_\beta^{\omega(1)} \end{pmatrix} \quad (46)$$

All elements of the matrices and vectors in eqs. 41–46 are again matrices or vectors themselves, and the orders indicated in superscripts (n) refer to Møller-Plesset perturbation theory order. The elements of these matrices or vectors were already defined in eqs. 12–25.

To evaluate the linear response function, the inhomogeneous system of equations in eq. 2 must again be solved. Assuming once more that the solution vector $\mathbf{X}_\beta(\omega)$ can be split into zeroth, first, and second-order contributions, and using the partitioning of the other vectors and matrices, eq. 2 can be rewritten as

$$\begin{aligned} \underbrace{\mathbf{T}(\hat{O}_\beta)^{[0]}}_{0\text{-order contribution}} + \underbrace{\mathbf{T}(\hat{O}_\beta)^{[1]}}_{1\text{st-order contribution}} &= \underbrace{(\omega \mathbf{S}^{[0]} - \mathbf{E}^{[0]}) \mathbf{X}_\beta(\omega)^{[0]}}_{0\text{-order contribution}} \\ &+ \underbrace{(\omega \mathbf{S}^{[0]} - \mathbf{E}^{[0]}) \mathbf{X}_\beta(\omega)^{[1]} + (\omega \mathbf{S}^{[1]} - \mathbf{E}^{[1]}) \mathbf{X}_\beta(\omega)^{[0]}}_{1\text{st-order contribution}} \\ &+ \underbrace{(\omega \mathbf{S}^{[1]} - \mathbf{E}^{[1]}) \mathbf{X}_\beta(\omega)^{[1]} + (\omega \mathbf{S}^{[0]} - \mathbf{E}^{[0]}) \mathbf{X}_\beta(\omega)^{[2]}}_{2\text{nd-order contribution}} \\ &+ \dots \end{aligned} \quad (47)$$

As the full property gradient in this case is considered the sum of the zeroth and first-order contributions, any second-order contribution to the full property gradient must be 0. The equation can thus be split up into the following zeroth, first, and second-order equations, where eqs. 41–46 can be inserted.

As seen in the derivation of the RPA(D) model, the form of the zeroth-order property gradient allows the zeroth-order equation to be written compactly, as only the single excitation part of the problem is nonzero:

$$\begin{pmatrix} \omega(\mathbf{1} + \boldsymbol{\Sigma}^{(2)}) - \mathbf{A}^{(0,1,2)} & -\mathbf{B}^{(1,2)} \\ -\mathbf{B}^{(1,2)} & -\omega(\mathbf{1} + \boldsymbol{\Sigma}^{(2)}) - \mathbf{A}^{(0,1,2)} \end{pmatrix} \begin{pmatrix} e\mathbf{X}_\beta^{\omega[0]} \\ d\mathbf{X}_\beta^{\omega[0]} \end{pmatrix} = \begin{pmatrix} e\mathbf{O}_\beta^{\omega(0,2)} \\ d\mathbf{O}_\beta^{\omega(0,2)} \end{pmatrix} \quad (48)$$

Note that solving eq. 48 corresponds to solving the HRPDA problem.

Likewise, the first and second-order equations can be compactly written as

$$\begin{pmatrix} \omega\mathbf{1} - \mathbf{D}^{(0)} & 0 \\ 0 & -\omega\mathbf{1} - \mathbf{D}^{(0)} \end{pmatrix} \begin{pmatrix} e\Xi_\beta^{\omega[1]} \\ d\Xi_\beta^{\omega[1]} \end{pmatrix} = \begin{pmatrix} e\Omega_\beta^{\omega[1]} \\ d\Omega_\beta^{\omega[1]} \end{pmatrix} + \begin{pmatrix} \mathbf{C}^{(1)} & 0 \\ 0 & \mathbf{C}^{(1)} \end{pmatrix} \begin{pmatrix} e\mathbf{X}_\beta^{\omega[0]} \\ d\mathbf{X}_\beta^{\omega[0]} \end{pmatrix} \quad (49)$$

$$\begin{pmatrix} \omega(\mathbf{1} + \boldsymbol{\Sigma}^{(2)}) - \mathbf{A}^{(0,1,2)} & -\mathbf{B}^{(1,2)} \\ -\mathbf{B}^{(1,2)} & -\omega(\mathbf{1} + \boldsymbol{\Sigma}^{(2)}) - \mathbf{A}^{(0,1,2)} \end{pmatrix} \begin{pmatrix} e\mathbf{X}_\beta^{\omega[2]} \\ d\mathbf{X}_\beta^{\omega[2]} \end{pmatrix} = \begin{pmatrix} \tilde{\mathbf{C}}^{(1)} & 0 \\ 0 & \tilde{\mathbf{C}}^{(1)} \end{pmatrix} \begin{pmatrix} e\Xi_\beta^{\omega[1]} \\ d\Xi_\beta^{\omega[1]} \end{pmatrix} \quad (50)$$

It is observed that the first-order equation in this derivation is identical to the one obtained for the derivation of the RPA(D) model—that is, eq. 30 and 49 are identical.

By inserting the partitioned solution vector and property gradient in the expression for the linear response function, it is possible to obtain a new expression for the full linear response function evaluated through second order in pseudo-perturbation theory.

$$\begin{aligned} \langle\langle \hat{P}_\alpha; \hat{O}_\beta \rangle\rangle_\omega^{HRPA(D)} &= \mathbf{T}^T (\hat{P}_\alpha)^{[0]} \mathbf{X}_\beta(\omega)^{[0]} \\ &+ \mathbf{T}^T (\hat{P}_\alpha)^{[0]} \mathbf{X}_\beta(\omega)^{[1]} + \mathbf{T}^T (\hat{P}_\alpha)^{[1]} \mathbf{X}_\beta(\omega)^{[0]} \\ &+ \mathbf{T}^T (\hat{P}_\alpha)^{[0]} \mathbf{X}_\beta(\omega)^{[2]} + \mathbf{T}^T (\hat{P}_\alpha)^{[1]} \mathbf{X}_\beta(\omega)^{[1]} \quad (51) \end{aligned}$$

Again, all first-order contributions to the linear response function will be 0, due to the form of the zeroth and first-order vectors using the same arguments following eq. 36. The zeroth-order contribution will simply be the HRPDA linear response function, while the second-order contribution offers a correction. By once again utilizing that a left-hand side zeroth-order solution vector can be defined, now as

$$\begin{aligned} (e\mathbf{X}_\alpha^{\omega[0]T} d\mathbf{X}_\alpha^{\omega[0]T}) &= (e\mathbf{P}_\alpha^{(0,2)} d\mathbf{P}_\alpha^{(0,2)}) \\ &\times \left(\begin{pmatrix} \omega(\mathbf{1} + \boldsymbol{\Sigma}^{(2)}) - \mathbf{A}^{(0,1,2)} & -\mathbf{B}^{(1,2)} \\ -\mathbf{B}^{(1,2)} & -\omega(\mathbf{1} + \boldsymbol{\Sigma}^{(2)}) - \mathbf{A}^{(0,1,2)} \end{pmatrix} \right)^{-1} \quad (52) \end{aligned}$$

the second order linear response function at the HRPDA(D) level can be written

$$\langle\langle \hat{P}_\alpha; \hat{O}_\beta \rangle\rangle_\omega^{HRPA(D)} = \langle\langle \hat{P}_\alpha; \hat{O}_\beta \rangle\rangle_\omega^{HRPA(D),S} + \langle\langle \hat{P}_\alpha; \hat{O}_\beta \rangle\rangle_\omega^{HRPA(D),D} \quad (53)$$

$$\langle\langle \hat{P}_\alpha; \hat{O}_\beta \rangle\rangle_\omega^{HRPA(D),S} = (e\mathbf{P}_\alpha^{(0,2)} d\mathbf{P}_\alpha^{(0,2)}) \begin{pmatrix} e\mathbf{X}_\beta^{\omega[0]} \\ d\mathbf{X}_\beta^{\omega[0]} \end{pmatrix} = \langle\langle \hat{P}_\alpha; \hat{O}_\beta \rangle\rangle_\omega^{HRPA} \quad (54)$$

$$\begin{aligned} \langle\langle \hat{P}_\alpha; \hat{O}_\beta \rangle\rangle_\omega^{HRPA(D),D} &= - (e\mathbf{X}_\alpha^{\omega[0]T} d\mathbf{X}_\alpha^{\omega[0]T}) \begin{pmatrix} \tilde{\mathbf{C}}^{(1)} & 0 \\ 0 & \tilde{\mathbf{C}}^{(1)} \end{pmatrix} \begin{pmatrix} \mathbf{D}^{(0)} - \omega\mathbf{1} & 0 \\ 0 & \omega\mathbf{1} + \mathbf{D}^{(0)} \end{pmatrix}^{-1} \\ &\times \left\{ \begin{pmatrix} e\Omega_\beta^{\omega(1)} \\ d\Omega_\beta^{\omega(1)} \end{pmatrix} + \begin{pmatrix} \mathbf{C}^{(1)} & 0 \\ 0 & \mathbf{C}^{(1)} \end{pmatrix} \begin{pmatrix} e\mathbf{X}_\beta^{\omega[0]} \\ d\mathbf{X}_\beta^{\omega[0]} \end{pmatrix} \right\} \\ &- (e\mathbf{P}_\alpha^{(1)} d\mathbf{P}_\alpha^{(1)}) \begin{pmatrix} \mathbf{D}^{(0)} - \omega\mathbf{1} & 0 \\ 0 & \omega\mathbf{1} + \mathbf{D}^{(0)} \end{pmatrix}^{-1} \\ &\times \left\{ \begin{pmatrix} e\Omega_\beta^{\omega(1)} \\ d\Omega_\beta^{\omega(1)} \end{pmatrix} + \begin{pmatrix} \mathbf{C}^{(1)} & 0 \\ 0 & \mathbf{C}^{(1)} \end{pmatrix} \begin{pmatrix} e\mathbf{X}_\beta^{\omega[0]} \\ d\mathbf{X}_\beta^{\omega[0]} \end{pmatrix} \right\} \\ &= \langle\langle \hat{P}_\alpha; \hat{O}_\beta \rangle\rangle_\omega^{RPA(D),D} \quad (55) \end{aligned}$$

It is observed that the double excitation part of the polarization propagators are identical for RPA(D) and HRPDA(D) eqs. 39 and 55.

Computational cost of doubles corrected methods

While both RPA(D) and HRPDA(D) are approximations to SOPPA with reduced cost, the extend to which the cost is reduced differs. Thus, it is worthwhile to briefly discuss the cost of these methods in terms of the number of occupied orbitals, O , the number of basis functions, N , and the number of virtual orbitals, $V = N - O$. The cost of calculating the RPA equations scales with the fourth power of the size of the basis set (N^4). The leading terms in the SOPPA approach on the other hand scales as a partial two-electron integrals transformation, N^4O .¹ As all of the methods presented here require transformation with the SOPPA matrices, they all have N^4O as their highest scaling term.

In RPA(D) only the RPA equations are solved iteratively and the N^4O contribution are calculated once using the converged RPA vectors. The savings of RPA(D) relative to SOPPA for a large system should be proportional to the number of iterations required to converge the SOPPA equations. HRPDA(D) on the other hand requires the iterative solution of the HRPDA equations, which includes the most computationally costly part of the SOPPA matrix, the $\mathbf{B}^{(2)}$ matrix. A HRPDA iteration thus requires the same amount of N^4O terms as a SOPPA iteration, though the calculation of some N^3O^2 and NV^2O^2 terms can be avoided. The savings of HRPDA in terms of the computational cost of an iteration is thus quite small in the typical case of $V \gg O$, but solving a system of linear equations of singles size may still be considerably easier than one of full singles and doubles size.

¹ Or in V^4O in an MO based approach, however, this would require storing all integrals and performing a full N^5 integral transformation.

Implementation of the RPA(D) and HRP(A) Models

The RPA(D) and HRP(A) models have been implemented in the atomic integral direct SOPPA module^[34,48] of the DALTON program.^[49]

To implement the RPA(D) model the two contributions in eqs. 39–40 are investigated further separately. Considering first the single excitation part of the linear response function $\langle\langle \hat{P}_{ai}; \hat{O}_{\beta}^{\omega} \rangle\rangle_{\omega}^{RPA(D),S}$ in eq. 39, this can be rewritten as follows:

$$\begin{aligned} & \langle\langle \hat{P}_{ai}; \hat{O}_{\beta}^{\omega} \rangle\rangle_{\omega}^{RPA(D),S} \\ &= \mathbf{T}^T(\hat{P}_{\alpha})^{[0]} \mathbf{X}_{\beta}^{\omega[0]} + \mathbf{X}_{\alpha}^{\omega[0]} \mathbf{T}(\hat{O}_{\beta}^{\omega})^{[2]} + \mathbf{T}^T(\hat{P}_{\alpha})^{[2]} \mathbf{X}_{\beta}^{\omega[0]} \\ & \quad + \mathbf{X}_{\alpha}^{\omega[0]} (\mathbf{E}^{[2]} - \omega \mathbf{S}^{[2]}) \mathbf{X}_{\beta}^{\omega[0]} \\ &= \mathbf{T}^T(\hat{P}_{\alpha})^{[0]} \mathbf{X}_{\beta}^{\omega[0]} + \mathbf{X}_{\alpha}^{\omega[0]} \left\{ \mathbf{T}(\hat{O}_{\beta}^{\omega})^{[2]} + \frac{1}{2} (\mathbf{E}^{[2]} - \omega \mathbf{S}^{[2]}) \mathbf{X}_{\beta}^{\omega[0]} \right\} \\ & \quad + \left\{ \frac{1}{2} \mathbf{X}_{\alpha}^{\omega[0]} (\mathbf{E}^{[2]} - \omega \mathbf{S}^{[2]}) + \mathbf{T}^T(\hat{P}_{\alpha})^{[2]} \right\} \mathbf{X}_{\beta}^{\omega[0]} \\ &= \mathbf{X}_{\alpha}^{\omega[0]} \left\{ \mathbf{T}(\hat{O}_{\beta}^{\omega})^{[0,2]} + \frac{1}{2} (\mathbf{E}^{[0,2]} - \omega \mathbf{S}^{[0,2]}) \mathbf{X}_{\beta}^{\omega[0]} \right\} \\ & \quad + \left\{ \frac{1}{2} \mathbf{X}_{\alpha}^{\omega[0]} (\mathbf{E}^{[0,2]} - \omega \mathbf{S}^{[0,2]}) + \mathbf{T}^T(\hat{P}_{\alpha})^{[0,2]} \right\} \mathbf{X}_{\beta}^{\omega[0]} \quad (56) \end{aligned}$$

To implement the RPA(D) linear response function, it is necessary first to run an RPA calculation and to save the RPA solution vectors $\mathbf{X}_{\alpha}^{\omega[0]}$ and $\mathbf{X}_{\beta}^{\omega[0]}$. The single excitation part of the RPA(D) linear response function is thus calculated in the following steps:

- The vector $\mathbf{Y}_{\alpha} = (\mathbf{E}^{[0,2]} - \omega \mathbf{S}^{[0,2]}) \mathbf{X}_{\alpha}^{\omega[0]}$ and the equivalent \mathbf{Y}_{β} are determined for the single excitation part using existing routines for linear transformations of a vector with the $\mathbf{E}^{[0,2]}$ and $\mathbf{S}^{[0,2]}$ matrices.
- The vector $\mathbf{Z}_{1\alpha} = \mathbf{T}^T(\hat{P}_{\alpha})^{[0,2]} + \frac{1}{2} \mathbf{Y}_{\alpha}$ and the equivalent $\mathbf{Z}_{1\beta} = \mathbf{T}^T(\hat{O}_{\beta}^{\omega})^{[0,2]} + \frac{1}{2} \mathbf{Y}_{\beta}$ are determined for the single excitation part.
- The single excitation part of the RPA(D) linear response function is calculated as

$$\langle\langle \hat{P}_{ai}; \hat{O}_{\beta}^{\omega} \rangle\rangle_{\omega}^{RPA(D),S} = \mathbf{X}_{\alpha}^{\omega[0]} \mathbf{Z}_{1\beta} + \mathbf{Z}_{1\alpha} \mathbf{X}_{\beta}^{\omega[0]} \quad (57)$$

Considering the double excitation part of the linear response function $\langle\langle \hat{P}_{ai}; \hat{O}_{\beta}^{\omega} \rangle\rangle_{\omega}^{RPA(D),D}$ given in eq. 40, we obtain:

$$\begin{aligned} & \langle\langle \hat{P}_{ai}; \hat{O}_{\beta}^{\omega} \rangle\rangle_{\omega}^{RPA(D),D} = -\mathbf{X}_{\alpha}^{\omega[0]} \mathbf{E}^{[1]} (\mathbf{E}^{[0]} - \omega \mathbf{S}^{[0]})^{-1} \left\{ \mathbf{T}(\hat{O}_{\beta}^{\omega})^{[1]} + \mathbf{E}^{[1]} \mathbf{X}_{\beta}^{\omega[0]} \right\} \\ & \quad - \mathbf{T}^T(\hat{P}_{\alpha})^{[1]} (\mathbf{E}^{[0]} - \omega \mathbf{S}^{[0]})^{-1} \left\{ \mathbf{T}(\hat{O}_{\beta}^{\omega})^{[1]} + \mathbf{E}^{[1]} \mathbf{X}_{\beta}^{\omega[0]} \right\} \end{aligned}$$

$$\begin{aligned} &= -\left\{ \mathbf{X}_{\alpha}^{\omega[0]} \mathbf{E}^{[1]} + \mathbf{T}^T(\hat{P}_{\alpha})^{[1]} \right\} (\mathbf{E}^{[0]} - \omega \mathbf{S}^{[0]})^{-1} \\ & \quad \times \left\{ \mathbf{T}(\hat{O}_{\beta}^{\omega})^{[1]} + \mathbf{E}^{[1]} \mathbf{X}_{\beta}^{\omega[0]} \right\} \quad (58) \end{aligned}$$

Defining the vectors $\mathbf{Z}_{2\alpha} = \mathbf{T}^T(\hat{P}_{\alpha})^{[1]} + \mathbf{X}_{\alpha}(\omega)^{[0]} \mathbf{E}^{[1]}$ and $\mathbf{Z}_{2\beta} = \mathbf{T}(\hat{O}_{\beta}^{\omega})^{[1]} + \mathbf{E}^{[1]} \mathbf{X}_{\beta}(\omega)^{[0]}$ eq. 58 can be written:

$$\langle\langle \hat{P}_{ai}; \hat{O}_{\beta}^{\omega} \rangle\rangle_{\omega}^{RPA(D),D} = -\mathbf{Z}_{2\alpha} (\mathbf{E}^{[0]} - \omega \mathbf{S}^{[0]})^{-1} \mathbf{Z}_{2\beta} \quad (59)$$

Equation 59 was implemented in the DALTON program using that the inversion of the $(\mathbf{E}^{[0]} - \omega \mathbf{S}^{[0]})$ matrix is trivial due to its diagonal form. Finally, the linear response function at the RPA(D) level is calculated as the sum of the single and double excitation contributions as stated in eq. 38.

HRPA(D)

The HRP(A) model was implemented by modifying the routine for the calculation of the linear response function using the RPA(D) model. As for the RPA(D) implementation, the calculation of the single excitation and double excitation contributions have been implemented separately to enable comparison of the magnitude of the contributions. As the single excitation part of the HRP(A) linear response function is just the HRP(A) linear response function, this contribution is found by multiplying the calculated HRP(A) solution vector, $\mathbf{X}_{\beta}(\omega)^{[0]}$, with the left-hand side single excitation property gradient. While of zeroth-order in pseudo-perturbation theory, the contributions are evaluated through second order for Møller-Plesset perturbation theory. The double excitation part of the HRP(A) model is identical to the one obtained for the RPA(D) model. The implementation of the double excitation part of the RPA(D) linear response function is thus used for the HRP(A) calculation as well. The only difference between the double excitation part of the RPA(D) and HRP(A) models lies in the zeroth-order solution vector used, that is, whether the RPA or HRP(A) solution vector is needed. The correct solution vector is in both cases obtained by running an RPA or HRP(A) calculation prior to the evaluation of the equations presented in this section.

Computational Details

Indirect nuclear spin-spin coupling constants have been calculated for the twenty molecules shown in Table 1, using a local development version of the DALTON program^[49] for the RPA, RPA(D), HRP(A), and HRP(A) models with the default convergence criterion. SOPPA and reference CCSD results have been taken from the literature.^[22] The CCSD results have been chosen as a reference, as these were the results at the highest level of theory available from literature for the chosen set of molecules. The CCSD method however, is not the most accurate in existence and calculations have been performed on some molecules at the CC3 and CCSDT levels, for example, H₂O^[11,14] and

Table 1. Molecules and couplings investigated in this study from Kjær et al.^[22]

Molecule	$^1J(XY)$	$^2hJ(XY)$	$^1J(XH)$	$^1hJ(XH)$	$^2J(HH)$
C ₂ H ₆	(C-C)	-	-	-	-
CH ₃ F	(C-F)	-	-	-	-
CH ₃ NH ₂	(C-N)	-	-	-	-
CH ₃ OH	(C-O)	-	(O-H)	-	-
CH ₄	-	-	(C-H)	-	(H-H)
F ₂ H ₂	-	(F-F)	-	-	-
F ₂ H ₃ ⁺	-	(F-F)	(F-H)	(F-H)	-
FHF ⁻	-	(F-F)	(F-H)	(F-H)	-
HF	-	-	(F-H)	-	-
H ₂ F ⁺	-	-	(F-H)	-	(H-H)
H ₂ N ⁻	-	-	(N-H)	-	(H-H)
H ₂ O	-	-	(O-H)	-	(H-H)
H ₃ O ⁺	-	-	(O-H)	-	(H-H)
OH ⁻	-	-	(O-H)	-	-
N ₂ H ₄	(N-N)	-	-	-	-
NF ₃	(N-F)	-	-	-	-
NH ₂ F	(N-F)	-	-	-	-
NH ₃ F ⁻	-	(N-F)	(N-H)	(F-H)	-
NH ₃	-	-	(N-H)	-	(H-H)
NH ₄ ⁺	-	-	(N-H)	-	(H-H)

HF.^[11] The effect on these two molecules of using the CCSDT or CC3 methods rather than the CCSD method was shown to be between approximately 0.5 Hz and 2 Hz, though for other molecules the residual was larger.^[11,14]

For comparisons of calculation time, SOPPA calculations were also performed using the local development version of DALTON. Note that, the timings are only approximate as it was not possible to control which other calculations were run simultaneously with the ones given here. Also, not all calculations were run on the same node.

To enable comparisons with results from the literature, the ccJ-pVTZ basis set^[50] has been used as in Kjær et al.,^[22] as well as the same geometries. The triple zeta basis was previously shown to yield sufficiently accurate results for a range of SOPPA and Coupled Cluster-based models.^[22,51] The added tight functions in the ccJ-pVTZ basis set make it well suited for calculations of magnetic properties, such as indirect nuclear spin–spin coupling constants; indeed it was optimized for this type of properties.^[50] Observe in Table 1 that for F₂H₃⁺ and FHF⁻ there are formally both an ordinary one-bond XY coupling and a one-bond XH coupling across a hydrogen bond. However, due to symmetry of the molecules, these two types of couplings are identical. Thirty-two different couplings will therefore be investigated in the following section. Note that, it is the ¹⁵N isotope that has been investigated. As a range of different couplings with widely varying values are investigated, comparisons will be done using the relative deviations of the results from the chosen reference.

Of the Thirty-two couplings seven are of the one-bond XY-type, that is, $^1J(XY)$ and four are two-bond XY coupling across a hydrogen bond, that is, $^2hJ(XY)$. Here X and Y refer to any non-Hydrogen atom. There are 11 $^1J(XH)$ couplings, that is, one bond XH couplings as well as three one-bond XH couplings across a hydrogen bond— $^1hJ(XH)$. Finally, seven two-bond HH bonds, $^2J(HH)$ couplings will be investigated. Both the number

of bonds, the coupling spans as well as the number of electrons in the vicinity of the involved nuclei influence the indirect nuclear spin–spin coupling constant. More electrons will for instance, result in a larger electron correlation effect, which is thus expected to play the largest role for couplings of the XY-type. Due to these differences the couplings will be investigated separately.

Results and Discussion

All couplings

Thirty-two different indirect nuclear spin–spin coupling constants have been calculated as well as their corresponding contributions. A comparison of the obtained results (i.e., all the full isotropic coupling constants as well as the PSO, SD, and FC-contributions) with the CCSD results from Kjær et al.,^[22] is shown in Figure 1. Note that, the statistics shown in Figure 1 as well as Table 2 includes all PSO, SD, and FC-contributions in addition to the total isotropic coupling constants to minimize the effects of error cancellation possibly contained in the total isotropic coupling constant from adding up the contributions.

The set of couplings investigated contain a wide range of couplings, many of which however, are couplings to F, O, and N. These often have large correlation contributions, and some models, such as RPA, therefore have difficulties describing them, as also remarked upon in Kjær et al.^[22]

A sign change was observed in two FC-terms upon doubles correction of the RPA model; the one obtained for the F-F coupling in F₂H₂, that is, F₂H₂(F-F), as well as the one obtained for H₂F(H-H). As the FC-term is the dominant contribution for the couplings investigated here, a large error in this term can lead to a very large error in the total isotropic coupling constant. Note that erroneous RPA results for this contribution can cause errors of RPA(D) results to explode for the total isotropic coupling constant. This was seen for a calculation of the N-O coupling in NH₂OH, where the relative deviation of the RPA calculated FC-term was 0.15 resulting in a relative deviation of the total isotropic coupling constant of 3, while the relative deviations for the RPA(D) model were 3 and 22, respectively. This coupling has therefore been removed from the set. No such problems were observed for HRPA and HRPA(D), where the relative deviations of the FC-term and the total isotropic coupling constant for both models were below 1.

For another four couplings, CH₃OH(O-H), CH₄(C-H), HF(F-H), and H₂O(O-H), the sign of the SD-contribution becomes correct compared to the CCSD results on going from RPA to RPA(D), that is, in the doubles corrected model. When considering the HRPA and HRPA(D) models, only one FC-term (F₂H₂(F-F)) was found to change its sign, while a change of sign was seen for the SD-term in three cases, CH₃OH(O-H), CH₄(C-H), and NH₃F⁻(N-H), two of which were already observed for RPA/RPA(D). Here, all changes of sign lead to the correct sign in the HRPA(D) calculations compared to the CCSD results.

As can be seen from Figure 1 and Table 2, the SOPPA model performs better compared to CCSD than all other models as expected, as this model solves the entire second-order problem

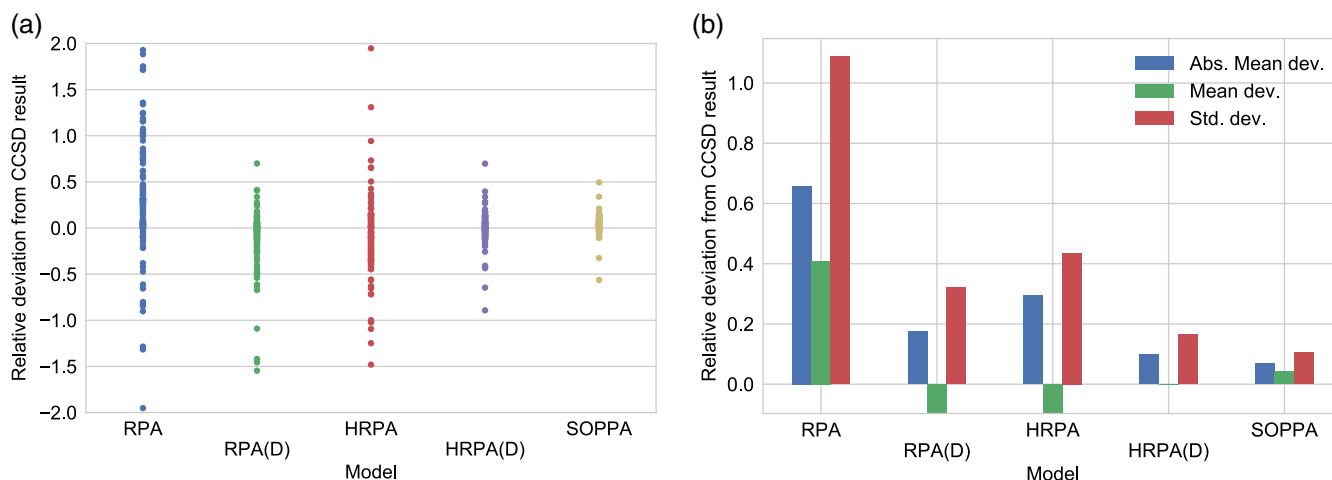


Figure 1. Relative deviations of all linear response properties from CCSD results calculated with ccJ-pVTZ basis set for 32 couplings, that is, all the full isotropic coupling constants as well as the PSO, SD, and FC contributions. A total of 128 linear response properties. The relative deviation was determined as $(J_i^{CCSD} - J_i^{Model})/J_i^{CCSD}$, where i is the total isotropic coupling constant or one of its contributions. Note that, several of the couplings and contributions to couplings for the RPA model are outside of the frame in (a). These are the SD-term of $\text{CH}_4(\text{C-H})$, $\text{NH}_4^+(\text{N-H})$ and $\text{HF}(\text{F-H})$, the FC-term of $\text{H}_2\text{F}^+(\text{H-H})$, $\text{CH}_3\text{NH}_2(\text{C-N})$, and $\text{F}_2\text{H}_2(\text{F-F})$ and finally the total coupling constant of $\text{H}_2\text{F}^+(\text{H-H})$ and $\text{H}_2\text{N}^-(\text{H-H})$. [Color figure can be viewed at wileyonlinelibrary.com]

Table 2. Absolute mean deviation and standard deviation of the relative deviations of the results of the investigated models from CCSD results calculated with ccJ-pVTZ basis set.

Model	Abs. mean dev.	Mean dev.	Std. dev.
RPA	0.6579	0.4089	1.0883
RPA(D)	0.1744	-0.0974	0.3218
HRPA	0.2948	-0.0964	0.4355
HRPA(D)	0.0989	0.0002	0.1656
SOPPA	0.0689	0.0414	0.1048

The PSO, SD, and FC contributions have been included in the statistics in addition to the total isotropic coupling constants.

iteratively. In contrast, the RPA model solves the problem iteratively only through first order. It is thus no surprise that this model yields the least accurate results compared to CCSD. In fact, all the other models offer a vast improvement on the RPA model.

One finds that both the HRPA model and the RPA(D) model appear to underestimate the results with mean deviations of approximately -10%, whereas the remaining models seem to overestimate the results as in Table 2. The HRPA(D) model is observed to have a mean deviation of approximately 0 and thus no clear trend to over/underestimate can be found. From Figure 1 it looks as if the HRPA(D) model is almost as accurate as the SOPPA model. Likewise, the RPA(D) and HRPA models seem comparable in accuracy, with the RPA(D) model yielding the better results.

From Figure 1 and Table 2, it is evident that the HRPA(D) model offers a significant improvement over the HRPA model, while it is not quite as large as the one offered by the RPA(D) model on the RPA model. Whereas the RPA model has an absolute mean deviation approximately 4 times larger than that of the RPA(D) model, the HRPA model has an absolute mean deviation only 3 times as large as that of the HRPA(D) model. Likewise, the standard deviation is decreased by slightly more than a

factor of 3 from RPA to RPA(D), while the decrease is about a factor of 2.5 going from HRPA to HRPA(D). The smaller effect of the correction in the case of the HRPA model is not surprising, since it only consists in a correction from the double excitation part, while the RPA(D) model also includes a correction from the single excitation part. It is interesting to observe that the RPA(D) model appears to perform better for these couplings than the HRPA model. From Table 2, it is clear that the absolute mean deviation of the HRPA model is almost twice as large as that of the RPA(D) model. Likewise, the standard deviation is about 1.4 times larger for the HRPA model than for the RPA(D) model. This indicates the importance of the double excitation part of the SOPPA linear response function, as the HRPA model should give a better estimate of the single excitation part.

Although the increase in accuracy from RPA to RPA(D) is larger than the increase found from HRPA to HRPA(D), the better starting point of HRPA(D) allows this doubles corrected model to become comparable in accuracy to the SOPPA model, while the RPA(D) is still significantly less accurate. From Table 2, one can further see that the SOPPA model has an absolute mean deviation of only a third of that of the RPA(D) model, but about 2/3 of the one obtained for the HRPA(D) model. Likewise, the RPA(D) model has a standard deviation of about thrice that of the SOPPA model, while that of the HRPA(D) model is only about 3/5 larger than that of the SOPPA model. These same trends can also be identified for all individual contributions to the indirect nuclear spin-spin coupling constant (the DSO term is not investigated, as this is not calculated as a linear response property) as shown in Figure 2. All values can be found in the Supporting Information.

Turning to the individual contributions, one finds in Figure 2 that the distribution of the relative deviations is significantly smaller for the PSO-term than for the remaining contributions. Furthermore, the SOPPA and RPA(D) models seem to overestimate the PSO-term, which is recalled to be a singlet property, while the RPA, HRPA, and HRPA(D) models appear to

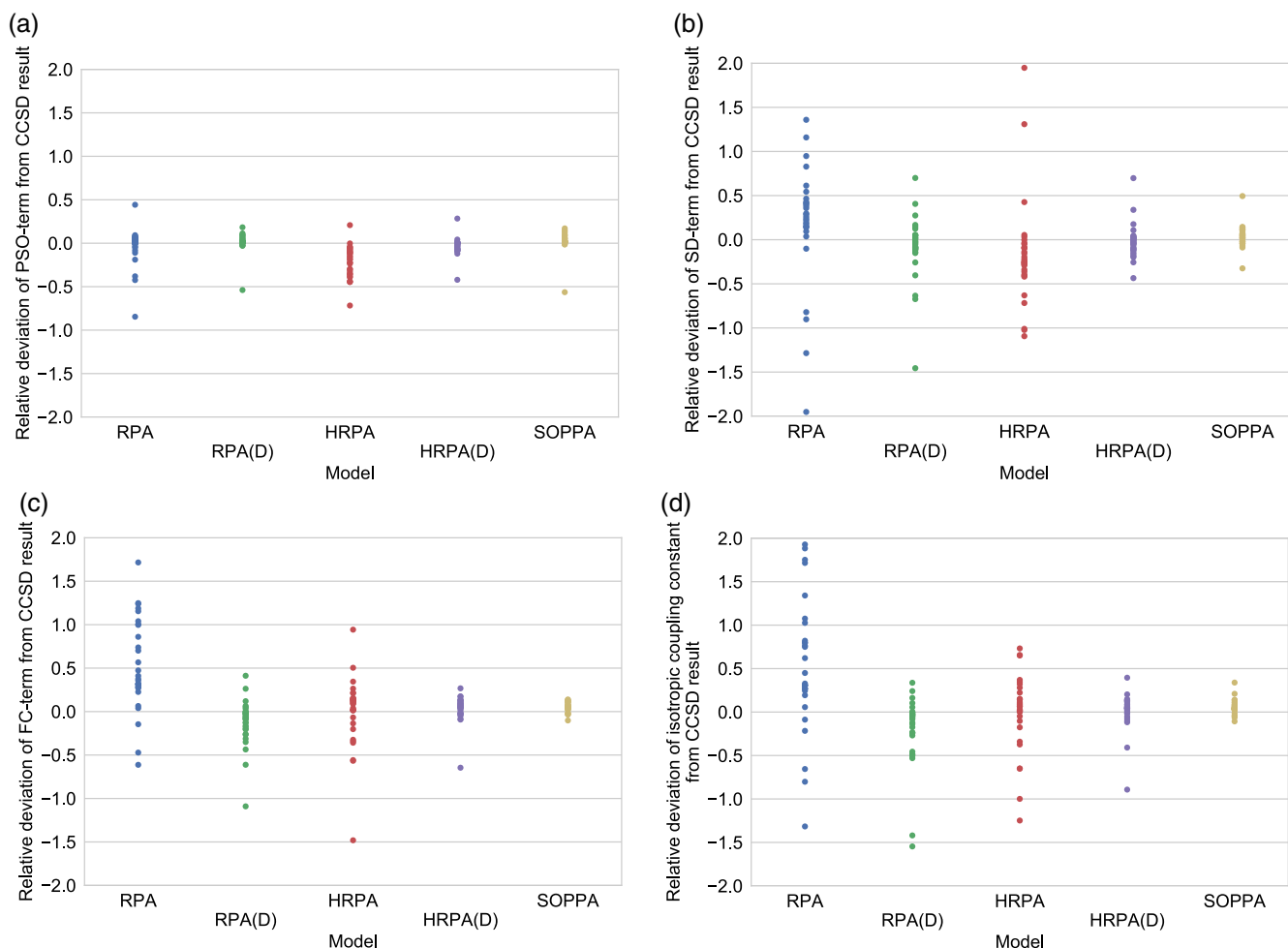


Figure 2. Relative deviations of individual contributions (a–c) and full isotropic coupling constant (d) from CCSD results. The relative deviation was determined as $(J_i^{CCSD} - J_i^{Model}) / J_i^{CCSD}$, where i is the total isotropic coupling constant or one of its contributions. All results were obtained using the cc-pVTZ basis set. Several RPA results are outside of the shown frame. (a) Relative deviation of PSO contribution from CCSD PSO contribution result. (b) Relative deviation of SD contribution from CCSD SD contribution results. For RPA $\text{CH}_4(\text{C-H})$, $\text{NH}_4^+(\text{N-H})$ and $\text{HF}(\text{F-H})$ are outside of the shown frame. (c) Relative deviation of FC contribution from CCSD FC contribution result. For RPA $\text{H}_2\text{F}^+(\text{H-H})$, $\text{CH}_3\text{NH}_2(\text{C-N})$ and $\text{F}_2\text{H}_2(\text{F-F})$ are outside of the shown frame. (d) Relative deviation of isotropic nuclear spin-spin coupling constant from CCSD calculated isotropic nuclear spin-spin coupling constant. $\text{H}_2\text{F}^+(\text{H-H})$ and $\text{H}_2\text{N}^-(\text{H-H})$ are outside of the shown frame for RPA. [Color figure can be viewed at wileyonlinelibrary.com]

underestimate this contribution. The mean deviation of the PSO, SD, and FC-terms as well as the total isotropic coupling constant can be found in Supporting Information. Calculations of singlet excitation energies carried out for the RPA, RPA(D), and SOPPA models^[34,36–39,47] as well as the HRPA model^[52] showed a general tendency of the RPA and HRPA models to overestimate the excitation energies, while the SOPPA and RPA(D) models generally underestimate singlet excitation energies. This is in complete agreement with the fact that methods that overestimate excitation energies, tend to underestimate response properties and vice versa.^[47]

In contrast to the singlet contributions, the RPA model seems to overestimate the triplet properties (FC-term and SD-term) with mean deviations of 40% and 60%, while the RPA(D) model underestimates these with mean deviations of –8% and –12%, respectively. The HRPA and HRPA(D) models appear to underestimate the SD-term, while they slightly overestimate the FC-term, the latter with mean deviations of approximately 0.2% and 4%. The SOPPA model slightly overestimates all

contributions in agreement with the trends previously shown for excitation energies.^[34–39,52] The RPA(D) model thus behaves differently than the RPA model, as also found in the calculations of triplet excitation energies,^[35] where the RPA model underestimated the results, while the RPA(D) model overestimated them, in agreement with the relationship between response properties and excitation energies.^[47] As previously mentioned, the RPA and hence RPA(D) models are prone to triplet instabilities leading to a wrong description of the properties. Such results are considered unstable, and when all these results obtained for the RPA model, were removed, the RPA(D) model was concluded to slightly underestimate the excitation energies in Haase et al.^[35] The reference was however, the CC3 model compared to which the CCSD model underestimated the results even more. Thus, compared to the CCSD reference used in this study, the RPA(D) model would overestimate triplet excitation energies, and hence be expected to underestimate the triplet linear response properties which is indeed the case. In the same study of triplet excitation energies, the HRPA model also

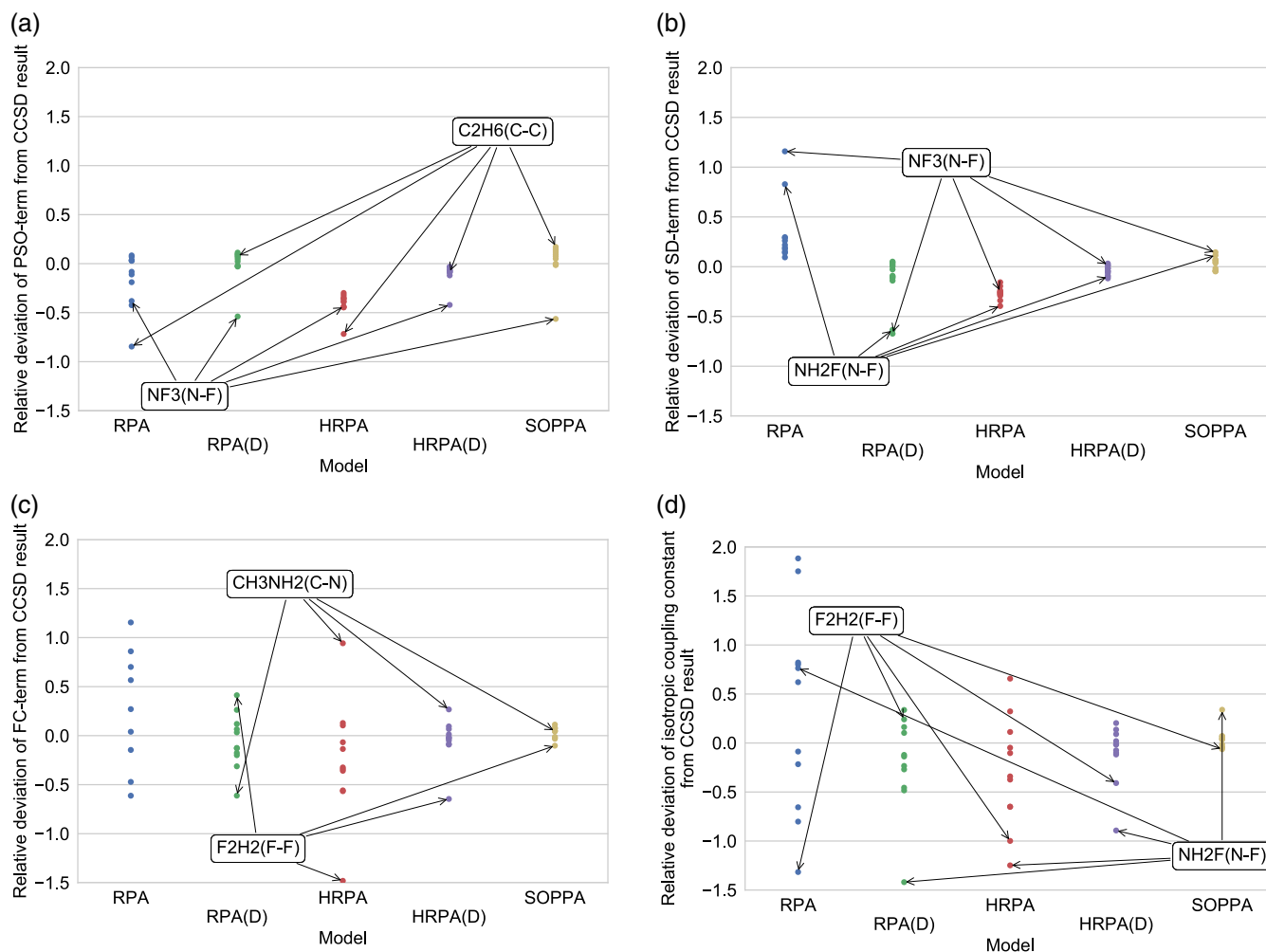


Figure 3. Relative deviations of individual contributions (a–c) and full isotropic coupling constant (d) of XY couplings from CCSD reference results. The relative deviation was determined as $(J_i^{CCSD} - J_i^{Model}) / J_i^{CCSD}$, where i is the total isotropic coupling constant or one of its contributions. All results were obtained using the ccJ-pVTZ basis set. Note that some RPA results are outside of the shown frame. (a) Relative deviation of PSO contribution from CCSD PSO contribution result. (b) Relative deviation of SD contribution from CCSD SD contribution result. (c) Relative deviation of FC contribution from CCSD FC contribution result. The contributions from F₂H₂(H-H) and CH₃NH₂(C-N) for the RPA model are outside of the shown frame. (d) Relative deviation of isotropic nuclear spin-spin coupling constant from CCSD calculated isotropic nuclear spin-spin coupling constant. [Color figure can be viewed at wileyonlinelibrary.com]

significantly overestimated the results. Hence, the HRP model would be expected to underestimate both triplet properties; however, this is only the case for the SD-term, while the FC-term is overestimated. This might be due to a difference in the chosen reference model or the different basis sets used. It could however, also be caused by too large differences between the types of molecules in the chosen benchmark sets.

From Figure 2d, it can be seen that the results for the total coupling are over or underestimated in accordance with the over or underestimation of the FC-term indicating that the dominating term is in fact the FC-term. Observe that relative deviations are considered, and thus the relative deviation of the total isotropic nuclear spin–spin coupling constant shown in Figure 2d is not the sum of the relative deviations of the contributions shown in Figures 2a–c.

To better investigate the models and understand the outliers, the couplings are split into three types and investigated separately in the following; XY couplings, one-bond XH couplings and two-bond HH couplings.

XY couplings

Seven of the thirty-two couplings are of the one-bond XY type as well as four two-bond XY couplings across a hydrogen bond. These are all collected in a single plot for XY couplings, and thus yield the plots shown in Figure 3. From this figure it can be seen that most of the outliers are caused by N-F or F-F couplings. As N and F both give rise to large correlation contributions,^[14] it is hardly surprising that the models have larger problems describing these particular couplings. Other outliers are observed, for example, the C-C coupling in C₂H₆ (PSO-term) and the C-N coupling in CH₃NH₂ (FC-term). While the first is only an outlier in the RPA and HRP models, the second is an outlier for all but the SOPPA model, however it seems to be more difficult for the RPA and HRP models than for the other models to describe this coupling, indicating the importance of the double excitation part for the linear response function. For these XY couplings, the models are seen to follow the

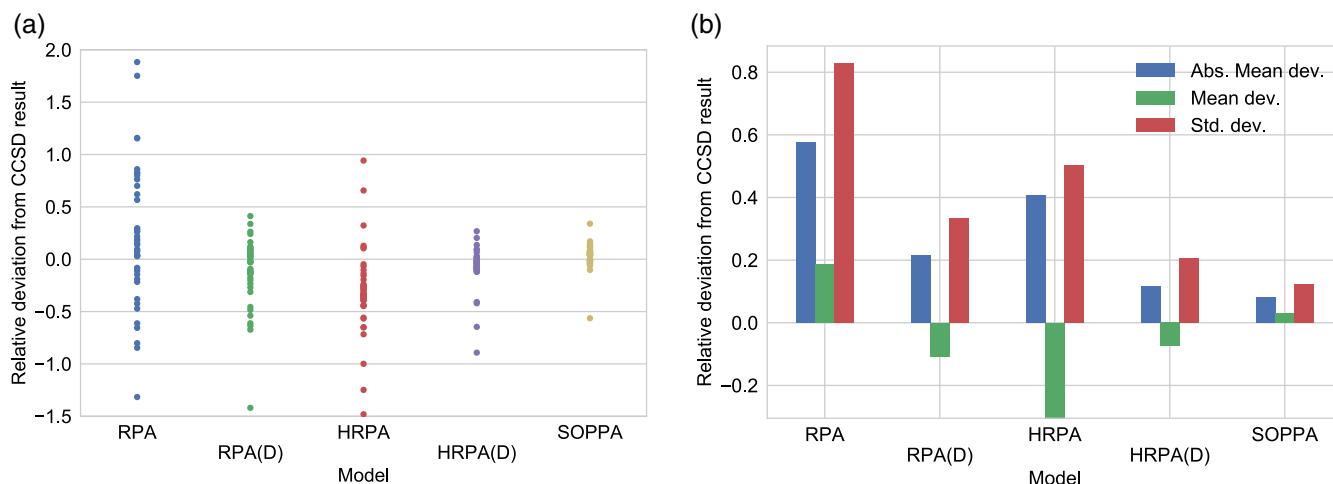


Figure 4. Relative deviation of XY couplings from CCSD reference results. All the full isotropic coupling constants as well as the PSO, SD and FC contributions have been included in the figure yielding a total of 44 values. The relative deviation was determined as $(J_i^{CCSD} - J_i^{Model})/J_i^{CCSD}$, where i is the total isotropic coupling constant or one of its contributions. All results were calculated using the ccJ-pVTZ basis set. Note that, the FC contributions of $F_2H_2(H-H)$ and $CH_3NH_2(C-N)$ for the RPA model are outside of the shown frame in (a). [Color figure can be viewed at wileyonlinelibrary.com]

same trends with respect to over/underestimation of the properties compared to CCSD as for all couplings. Note, that due to the outlier of the RPA(D) model the mean deviation for the PSO-term is negative, although only at -0.9% . Observe that for this set of XY couplings the HRP A model appears to underestimate all contributions, and so for triplet properties the HRP A and RPA(D) models behave in accordance with the behavior of the triplet excitation energy calculations in Haase et al.^[35] The HRP A(D) model seems to underestimate all the terms, though less so for the triplet property results.

Collecting all the linear response contributions of the coupling constant, that is, not the DSO-term, as well as the total isotropic nuclear spin–spin coupling constant in one plot yields Figure 4 and Table 3. Figure 4 and Table 3 leads to the same conclusions as for all couplings together. Thus, the RPA(D) model performs significantly better than the RPA model and surprisingly also the HRP A model, while still not being as accurate as the SOPPA model. The HRP A(D) model on the other hand is close to the SOPPA model in accuracy. For these XY-couplings it should be noted that the improvement the HRP A(D) model offers on the HRP A model, is larger than that offered by the RPA(D) model on the RPA model. This differs from the conclusions in the previous section, where all

Table 3. Absolute mean deviation and standard deviation of the relative deviations from the CCSD model of the investigated models using the ccJ-pVTZ basis set for 7 one-bond XY couplings and 4 two-bond XY couplings over a hydrogen bond.

Model	Abs. mean dev.	Mean dev.	Std. dev.
RPA	0.5764	0.1863	0.8271
RPA(D)	0.2146	−0.1069	0.3340
HRP A	0.4080	−0.3049	0.5028
HRP A(D)	0.1171	−0.0740	0.2057
SOPPA	0.0803	0.0317	0.1229

All the full isotropic coupling constants as well as the PSO, SD, and FC contributions have been included in the statistics.

couplings were considered. While HRP A(D) for the XY-couplings decreases the absolute mean deviation with approximately a factor of 4 from HRP A, the RPA(D) model only decreases this value with approximately a factor of 2.5 from RPA. The standard deviation however, is decreased about a factor of 2.5 by a doubles correction in both models.

The larger increase in accuracy for the HRP A(D) model might be due to a partial cancellation of the two corrections in the RPA(D) model. Due to the fairly small set of investigated XY-couplings, however, it might not be a general trend for all couplings of this type.

Furthermore, it should be observed that the outliers observed for both doubles corrected models, and in particular for HRP A(D), in Figure 4, seem to be among the largest observed in Figure 1. It should therefore be considered that the doubles corrected models seem to be ill-suited to describe couplings to fluorine cf. the section “Computational Details”.

One-bond XH couplings

Of the thirty-two couplings, fourteen are from one-bond XH couplings. Recall that three of these couplings are one-bond XH couplings across a hydrogen bond; the (F-H) couplings in FHF^- , $F_2H_3^+$, and NH_3F^- . Analyzing the contributions from all these one-bond XH couplings yields Figure 5. Again, it can be seen that the outliers mainly result from couplings with fluorine. In addition, the recurring coupling in question ($NH_3F(F-H)$) is across a hydrogen bond.

Once again, an outlier from another coupling is found, in this case an N-H coupling in NH_4^+ for the SD-term. This appears to affect all models except the RPA(D) model. It could be speculated that the only reason, it is not an outlier for the RPA(D) model, is error cancellation of the two corrections in this model.

For the investigated one-bond XH couplings the performance of each model seems stable, in the sense that the variance in the deviations of the results is fairly small for all models.

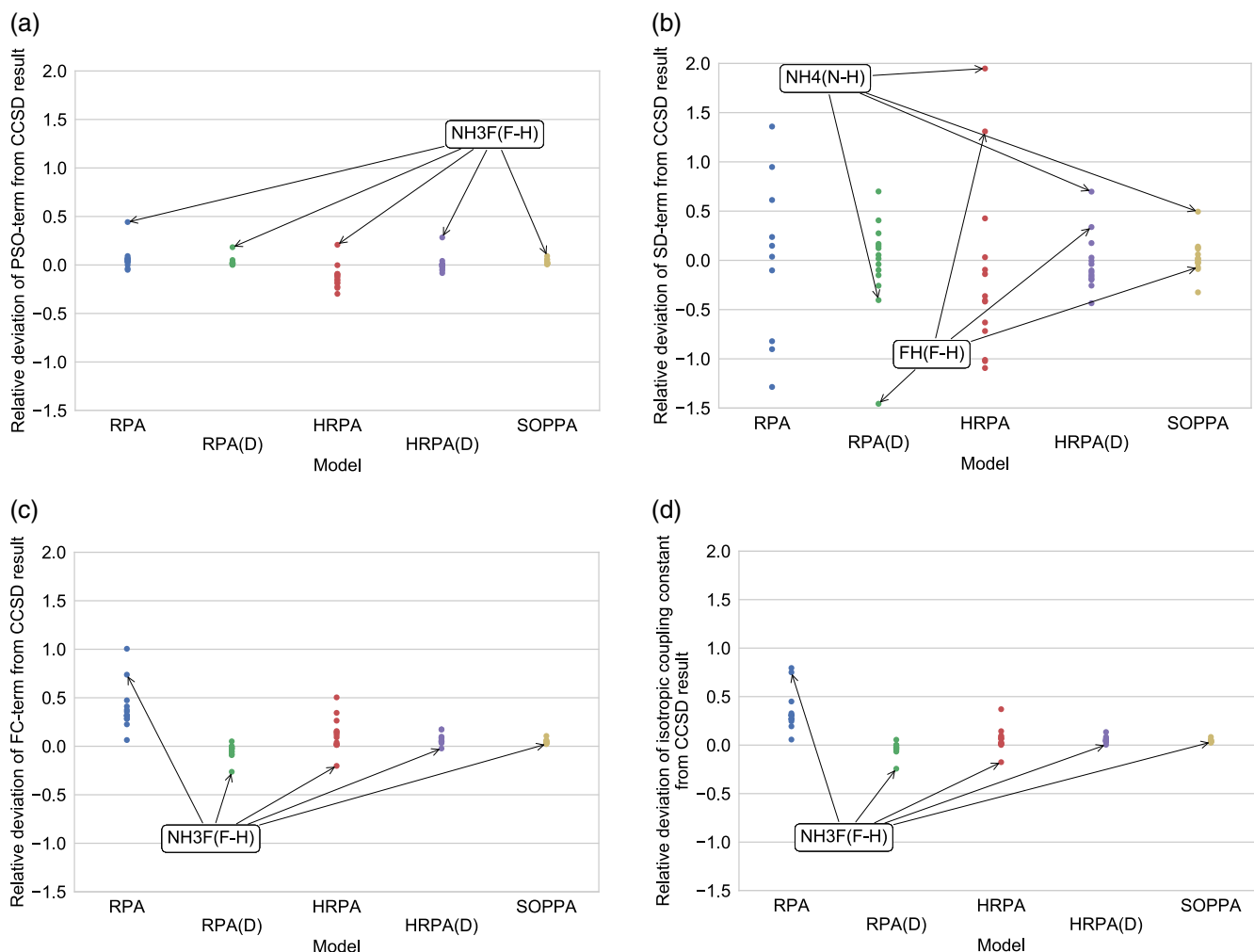


Figure 5. Relative deviations of individual contributions (a–c) and full isotropic coupling constant (d) of one-bond XH couplings from CCSD reference results. The relative deviation was determined as $(J_i^{CCSD} - J_i^{Model}) / J_i^{CCSD}$, where i is the total isotropic coupling constant or one of its contributions. All results were calculated using the cc-pVTZ basis set. The RPA results for the SD-terms of NH₄⁺(N-H), HF(F-H), CH₄(C-H) and CH₃OH(O-H) are outside of the shown frame. (a) Relative deviation of PSO contribution from CCSD PSO contribution result. (b) Relative deviation of SD contribution from CCSD SD contribution result. The RPA results for NH₄⁺(N-H), HF(F-H), CH₄(C-H) and CH₃OH(O-H) are outside of the shown frame. (c) Relative deviation of FC contribution from CCSD FC contribution result. (d) Relative deviation of isotropic nuclear spin-spin coupling constant from CCSD calculated isotropic nuclear spin-spin coupling constant. [Color figure can be viewed at wileyonlinelibrary.com]

The largest variance is found, not for the FC-term as seen for all couplings together, but rather for the SD-term. As this is generally not the dominating term for one-bond couplings, the results for the isotropic coupling constants show very little variance in the deviation for each model.

A possible explanation for the SD-term showing the most variance for these couplings could be that the values of this term is small compared to the remaining contributions as well as compared to the SD-terms of the XY-couplings.

As also observed for the XY-couplings, the RPA and HRP models perform significantly worse than the remaining models, which here appear to be of similar accuracy compared to CCSD. The doubles corrected models thus perform particularly well for this type of coupling.

The trends in over and underestimating the properties can be observed to be the same as previously noted.

If all contributions are investigated together, Figure 6 and Table 4 are obtained. One can conclude from Table 4 as well as

Figure 6 that once again, the HRP(D) model is comparable in accuracy to the SOPPA model for these couplings. In addition, the RPA(D) model also comes close to the SOPPA model in accuracy compared to the CCSD model. Whereas the HRP(D) model has a standard deviation about 1.5 times larger than that of the SOPPA model, the standard deviation of the RPA(D) model is only about 2.5 times as large as the one obtained for the SOPPA model. Both doubles corrected models have an absolute mean deviation approximately twice that of the SOPPA model. Thus, the RPA(D) model gives rise to a standard deviation of about 25%, while the SOPPA and HRP(D) models give rise to standard deviations of approximately 10% and 15%, respectively. Likewise, the absolute mean deviation is found to be 11% for the RPA(D) model, 6% for the SOPPA model, and 10% for the HRP(D) model.

It can be observed that all models seem to perform fairly well for the one-bond XH couplings compared to the performance for the XY-couplings. This could be a consequence of

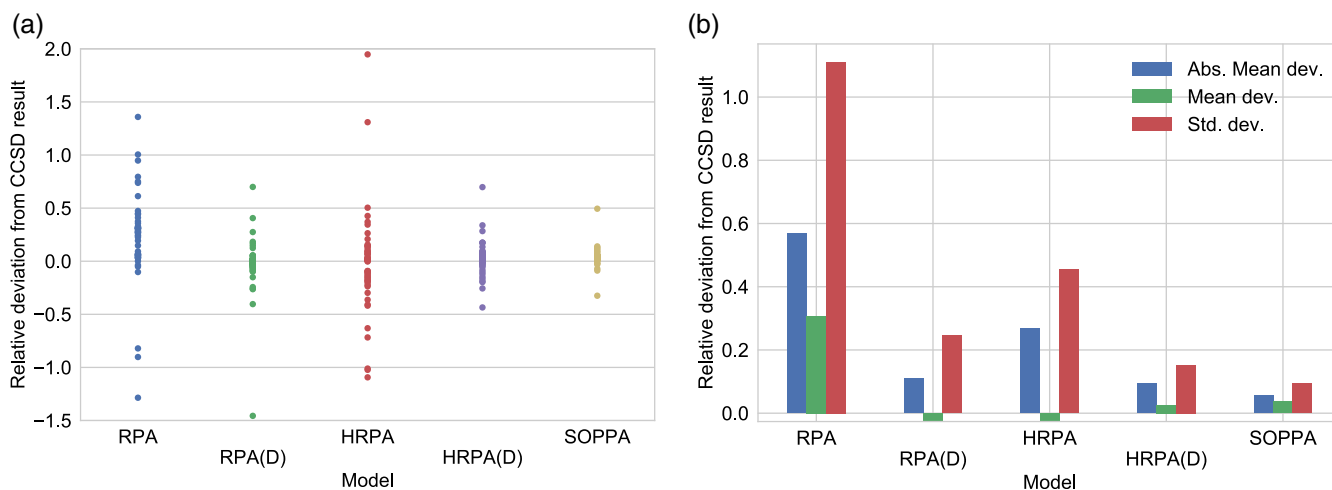


Figure 6. Relative deviation of one-bond XH couplings from CCSD reference results. All the full isotropic coupling constants as well as the PSO, SD, and FC contributions have been included in the figure yielding a total of 56 values. The relative deviation was determined as $(J_i^{CCSD} - J_i^{Model})/J_i^{CCSD}$, where i is the total isotropic coupling constant or one of its contributions. All results were calculated with the ccJ-pVTZ basis set. The RPA results for the SD-terms of NH_4^+ (N-H), HF(F-H), CH_4 (C-H), and CH_3OH (O-H) are outside of the shown frame on the left. [Color figure can be viewed at wileyonlinelibrary.com]

the lower percentage of couplings involving fluorine, which has already been observed to be problematic for the models to describe.

Two-bond HH couplings

Finally, the contributions of the remaining seven two-bond HH couplings are analyzed. This is shown in Figure 7, however as very few points are included, the outliers have not been marked. The outliers observed for RPA and RPA(D) are in all cases caused by the one fluorine containing molecule investigated for two-bond HH couplings.

From Figure 7, it can be seen that all models appear stable for the SD-term and in particular the PSO-term calculations. Slightly more variance is found in the deviations for the FC-term calculations, which can also be seen in the full isotropic coupling constant in Figure 7d, once again indicating that the FC-term is the dominating contribution to the full coupling constant. It should however be noted that the dominance of the FC-term for these couplings is mainly due to the PSO and DSO-terms being of more or less equal magnitude, but opposite sign. Thus, the two cancel out each other as also mentioned in

Kjær et al.^[22] While the trends in over and underestimation of the properties are the same as was observed for all couplings together, it should be noted that the RPA model vastly overestimates the triplet property terms which might indicate triplet instabilities.

Comparison of the methods for all linear response contributions and the total coupling constants are shown in Figure 8 and Table 5. Here, the RPA(D) model seems to perform worse than the HRPA model, while the HRPA(D) model yields results comparable to those obtained using the SOPPA model. Table 5 also shows that the SOPPA model yields the best results, however as also concluded from Figure 8, the HRPA(D) model yields results of almost the same accuracy. The standard deviation of the HRPA(D) model is only about 1/5 larger than that of the SOPPA model, and the absolute mean deviations of the two models are almost the same. Thus, the HRPA(D) model yields an absolute mean deviation of 8% and a standard deviation of approximately 11%, while the corresponding values for the SOPPA model are 8% and 9%, respectively.

It seems that for these couplings, an increase in accuracy follows from the size of the problem solved iteratively, that is, the accuracy is improved from RPA(D) over HRPA to HRPA(D). The RPA(D) model yields results with an absolute mean deviation about 1.5 times larger than the value obtained with the HRPA model. Likewise, the standard deviation is decreased with approximately a factor of two from RPA(D) to HRPA. Bearing in mind the few couplings investigated, this trend should be investigated further on a larger benchmark set.

The fact that the HRPA model appears to perform better than the RPA(D) model could indicate that the double excitation part of the linear response function is of less importance for this type of coupling than seen for the other two. However, the errors affecting the RPA model will of course also affect the RPA(D) model, thus making these results less reliable.

Table 4. Statistics on the relative deviations from CCSD results of the investigated models calculated using the ccJ-pVTZ basis set for 14 one-bond XH couplings.

Model	Abs. Mean Dev.	Mean Dev.	Std. Dev.
RPA	0.5691	0.3070	1.1112
RPA(D)	0.1100	-0.0235	0.2464
HRPA	0.2684	-0.0264	0.4546
HRPA(D)	0.0946	0.0263	0.1520
SOPPA	0.0562	0.0366	0.0944

All the full isotropic coupling constants as well as the PSO, SD, and FC contributions have been included in the statistics.

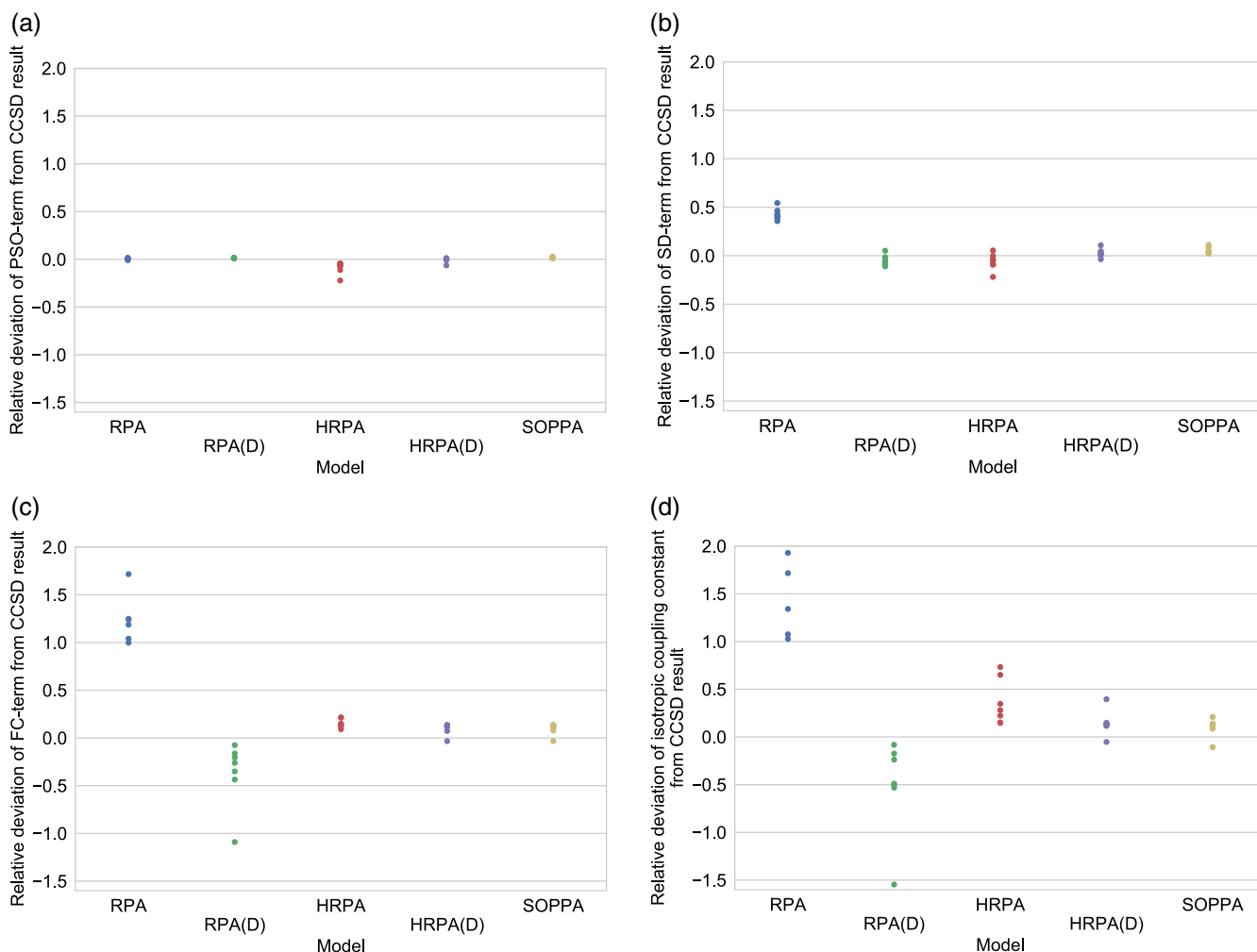


Figure 7. Relative deviations of individual contributions (a–c) and full isotropic coupling constant (d) of two-bond HH couplings from CCSD reference results. The relative deviation was determined as $(J_i^{CCSD} - J_i^{Model})/J_i^{CCSD}$, where i is the total isotropic coupling constant or one of its contributions. All results were obtained using the ccJ-pVTZ basis set. Several RPA results are outside of the shown frame. (a) Relative deviation of PSO contribution from CCSD PSO contribution result. (b) Relative deviation of SD contribution from CCSD SD contribution result. (c) Relative deviation of FC contribution from CCSD FC contribution result. $H_2F^+(H-H)$ is outside of the shown frame for RPA. (d) Relative deviation of isotropic nuclear spin-spin coupling constant from CCSD calculated isotropic nuclear spin-spin coupling constant. [Color figure can be viewed at wileyonlinelibrary.com]

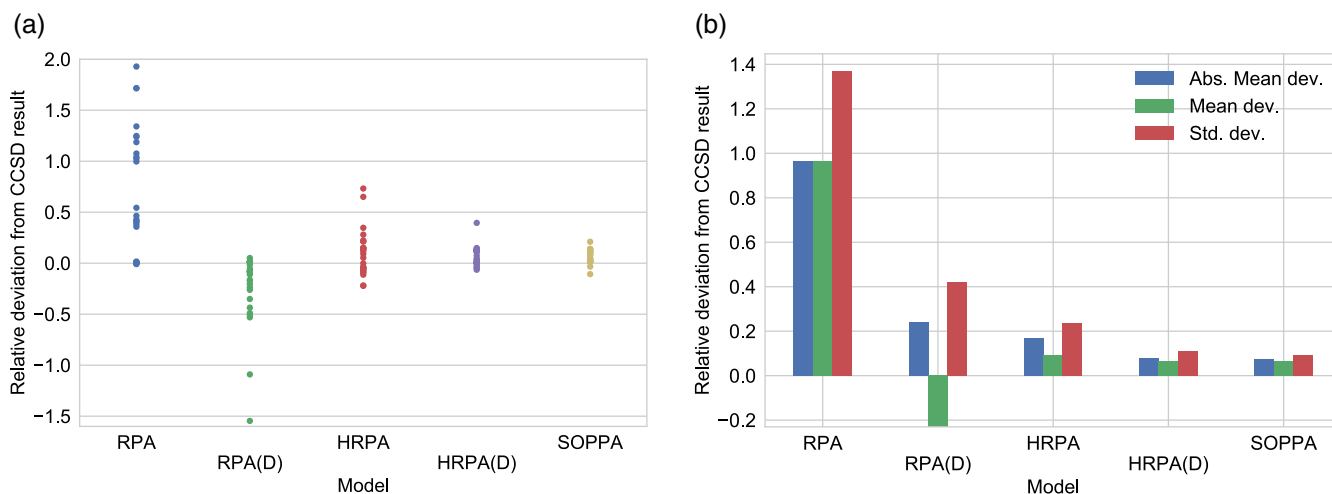


Figure 8. Relative deviation of two-bond HH couplings from CCSD reference results. All the full isotropic coupling constants as well as the PSO, SD and FC contributions have been included in the figure yielding a total of 28 values. The relative deviation was determined as $(J_i^{CCSD} - J_i^{Model})/J_i^{CCSD}$, where i is the total isotropic coupling constant or one of its contributions. All results were calculated with the ccJ-pVTZ basis set. The FC term for $H_2F^+(H-H)$ as well as the total isotropic coupling constant of $H_2F^+(H-H)$ and $H_2N^-(H-H)$ are outside of the shown frame for RPA on the left. [Color figure can be viewed at wileyonlinelibrary.com]

Table 5. Statistics on the relative deviations from CCSD results of the investigated models for 7 two-bond HH couplings.

Model	Abs. mean dev.	Mean dev.	Std. dev.
RPA	0.9636	0.9625	1.3675
RPA(D)	0.2401	-0.2301	0.4203
HRPA	0.1698	0.0911	0.2374
HRPA(D)	0.0789	0.0648	0.1124
SOPPA	0.0763	0.0663	0.0932

All results were calculated using the cc-j-pVTZ basis set. All the full isotropic coupling constants as well as the PSO, SD, and FC contributions have been included in the statistics.

Couplings without fluorine

As the couplings to fluorine and generally in fluorine containing molecules have proven difficult for all models to describe, the remaining 11 molecules without fluorine will briefly be investigated separately. These are shown in Figure 9. While little improvement is seen on the purely iterative models, that is, RPA, HRPA, and SOPPA, compared to Figure 1, the doubles corrected models are improved to show no outliers with relative deviations of 100% or more. We still, however, find deviations of up to around 65% for the two-doubles corrected methods and up to approximately 35% for SOPPA. These are quite large deviations and must be kept in mind when choosing a model for calculations. The largest deviations here are found for the triplet contributions and it might be that these are harder to describe using the models investigated in this study. Considering only the total indirect spin-spin coupling constant, outliers are still seen for all models, though the largest relative deviation is now at 50% for RPA(D), 40% for HRPA(D) and only 20% for SOPPA as seen from Figure 10. Note that, none of the outliers in the doubles corrected models are from one-bond XH couplings for which lower relative deviations are obtained.

Comparison with experiment

As the isotropic indirect nuclear spin-spin coupling constant is a measurable quantity, the obtained results should also be compared to experimental values.^[53–56] The 14 available experimental values are also given in the supporting information.

It must however, be considered that the theoretical results have not taken into account neither the vibrational effects, which can constitute up to 10% of the results,^[57–62] nor solvent effects.^[63,64] One must keep this in mind when comparing the results. This comparison is shown in Figure 11 and Table 6.

Interestingly, while the relative deviation of the RPA, HRPA, HRPA(D) and SOPPA results for approximately 60% of the couplings are increased compared to the values obtained with the CCSD model as a reference, only 50% are increased for the RPA(D) model. This might reflect that the RPA(D) model is the only model expected to underestimate these couplings based on the findings of the previous sections; as most of the included couplings are not of the XY-type, the HRPA model is not expected to underestimate the results. The general increase in the relative deviations is due to the fact that the CCSD model is expected to overestimate at least the triplet property contributions to the coupling constant.^[35] As the FC-term is the dominating term for this set of couplings, the CCSD model is thus expected to overestimate these couplings, consequently yielding too large relative deviations for the RPA(D) model. It might therefore be advantageous to further evaluate the models using a more accurate model, such as the CC3 model,^[11,14] as a reference. One can however still get a general idea of the model performances compared to one another using these results.

When considering the experimental values it is found that it is a coupling with fluorine that yields the outlier for RPA(D), SOPPA, and HRPA(D), while an additional outlier from the C-N coupling in CH₃NH₂ is observed for HRPA and RPA as well as

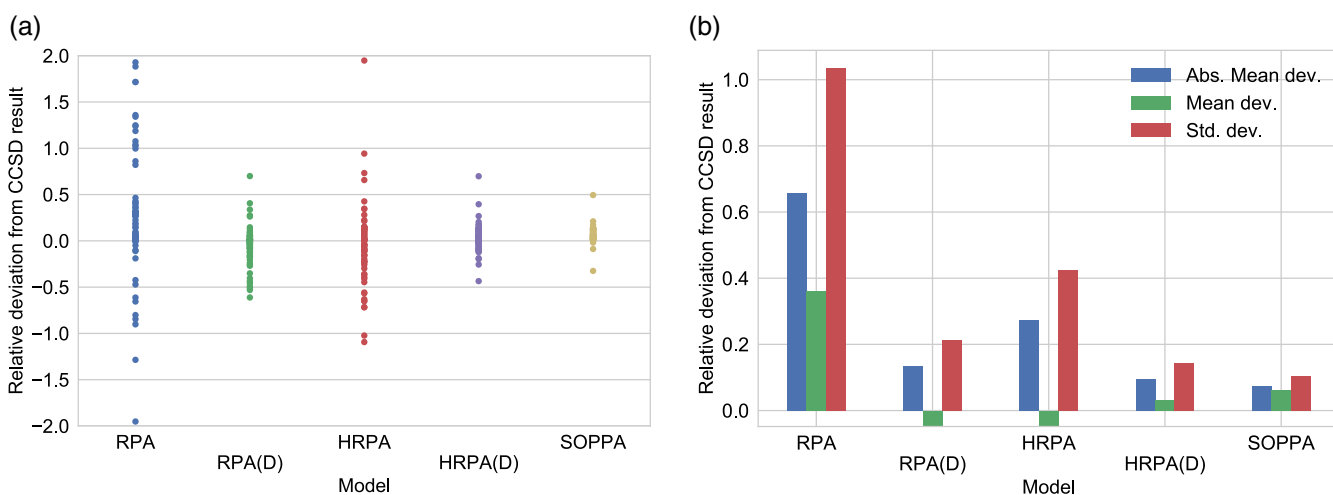


Figure 9. Relative deviations of all linear response properties from CCSD results calculated with the cc-j-pVTZ basis set for 18 couplings, that is, all the full isotropic coupling constants as well as the PSO, SD, and FC contributions yielding a total of 72 values. The relative deviation was determined as $(J_i^{CCSD} - J_i^{Model}) / J_i^{CCSD}$, where i is the total isotropic coupling constant or one of its contributions. The SD-terms of CH₄(C-H) and NH₄⁺(N-H), the FC-term of CH₃NH₂(C-N) and the total isotropic coupling constant of H₂N⁻(H-H) are outside of the shown frame for RPA in (a). [Color figure can be viewed at wileyonlinelibrary.com]

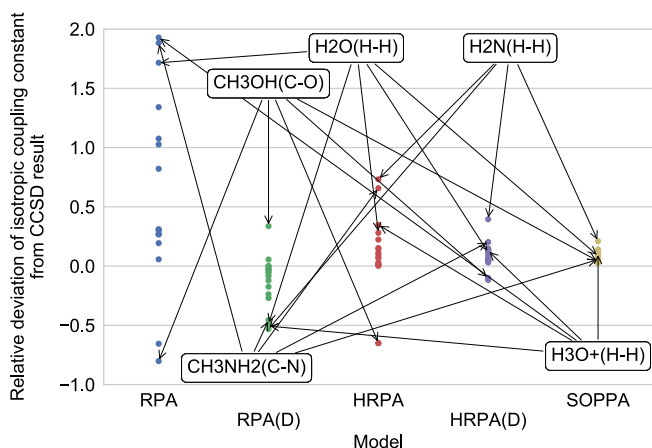


Figure 10. Relative deviation of the 18 total isotropic indirect nuclear spin-spin coupling constant from the 11 molecules containing no fluorine atoms calculated with the ccJ-pVTZ basis set. The relative deviation was determined as $(J_i^{CCSD} - J_i^{Model}) / J_i^{CCSD}$, where i is the total isotropic coupling constant. $H_2N^-(H-H)$ is outside of the shown frame for RPA. [Color figure can be viewed at wileyonlinelibrary.com]

HRPA(D), as also seen with CCSD as a reference for the FC-term. This would thus again indicate the importance of the double excitation part of the linear response function. Finally, the HRPA(D) model again seems to perform with an accuracy very close to that of the SOPPA model, for this sample of couplings, with both models yielding an absolute mean deviation and a standard deviation of approximately 13% and 19%, respectively, as can be seen in Table 6. The RPA(D) model also performs rather well for these couplings, though it is not as accurate as either the SOPPA or HRPA(D) model in comparison with experimental values. From Table 6, it can be observed that the RPA(D) model yields a standard deviation and an absolute mean deviation both about 1/4 larger than the values obtained for the HRPA(D) and SOPPA models.

It should be observed that the absolute mean deviation and standard deviation are larger for all models, except the RPA(D)

and HRPA models, compared to the results obtained with the CCSD model as a reference in Table 2. This might be a result of the missing vibrational effects; however, it could also be caused by the sample of couplings investigated in Figure 11 and Table 6 as opposed to all couplings in Figure 1 and Table 2.

The RPA model performs poorly compared to the experimental values with absolute mean deviation and standard deviation about six times larger than those obtained using the SOPPA model. The HRPA model performs better than the RPA model, with an absolute mean deviation about 1.5 times larger than for the SOPPA model and a standard deviation about 1.6 times larger. As the RPA(D) model still performs better, the importance of the double excitation part of the linear response function, can once again be noted.

Furthermore, it is observed that for this sample of couplings, the HRPA(D) model offers only a small improvement on the HRPA model compared to the improvement on the RPA model by a doubles correction. The doubles correction does however, in both cases increase the accuracy of the model significantly. Table 6 shows that the absolute mean deviation and standard deviation are decreased by approximately a third from HRPA to HRPA(D), while the decrease is approximately 4/5 from RPA to RPA(D).

Time requirements

After investigating the accuracy of the models compared to CCSD it is necessary to also consider the calculation time required for the new models. Figure 12 shows the calculation time of the two doubles corrected models in percentage of SOPPA calculation time for the investigated molecules. It is clear that the savings in time are significantly larger for the RPA(D) model compared to the HRPA(D) model. Furthermore, while an RPA(D) calculation can generally be expected to take approximately 25% of the time required for a SOPPA calculation, an HRPA(D) calculation might take anything from 30%–90% of the time required for a SOPPA calculation. The large

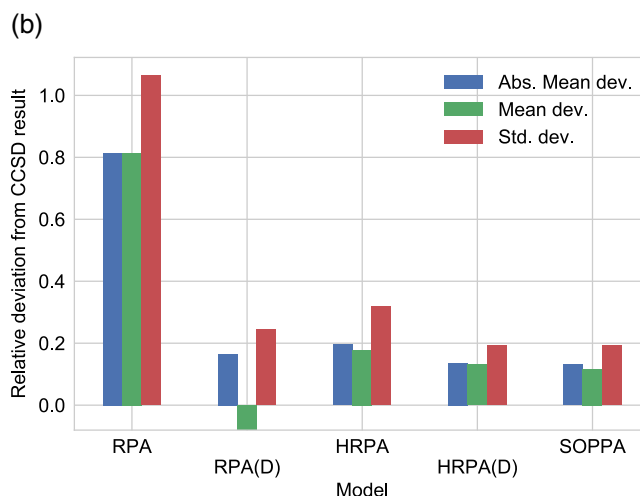
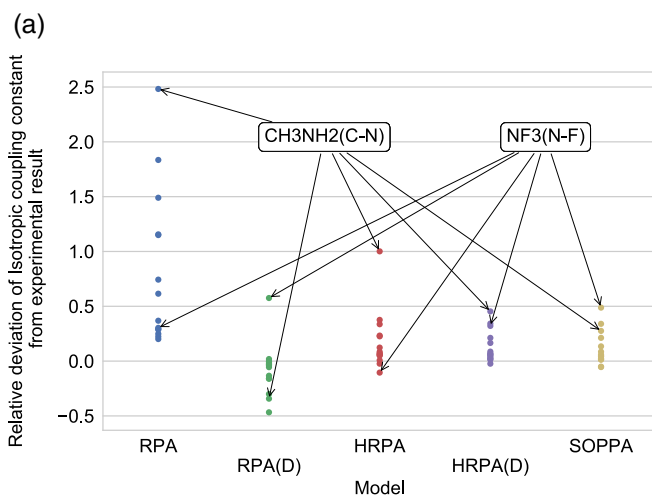


Figure 11. Analysis of relative deviation of isotropic nuclear spin-spin coupling constants from experimental values determined as $(J_i^{experiment} - J_i^{Model}) / J_i^{experiment}$, where i is the total isotropic nuclear spin-spin coupling constant. A total of 14 couplings are included. All results were obtained using the ccJ-pVTZ basis set. [Color figure can be viewed at wileyonlinelibrary.com]

Table 6. Absolute mean deviation and standard deviation of the relative deviations from the 14 experimental values of the total isotropic coupling constants of the investigated models.

Model	Abs. mean dev.	Mean dev.	Std. dev.
RPA	0.8141	0.8141	1.0652
RPA(D)	0.1654	-0.0806	0.2438
HRPA	0.1968	0.1785	0.3174
HRPA(D)	0.1357	0.1323	0.1930
SOPPA	0.1318	0.1168	0.1917

The ccJ-pVTZ basis set was used for the calculations.

variation for HRPA(D) might to some extent be due to the uncertainties caused by the lack of control with other calculations running simultaneously with the ones reported here.

Considering some statistics of the findings in Figure 12, we see that, while the minimum time requirement for the HRPA(D) model for the investigated molecules is comparable to the time requirements of the RPA(D) model, both the mean time requirement and the maximum time requirement are significantly larger than what is found for the RPA(D) model.

Considering the timings for three different molecules, we find, that for the RPA(D) model the savings in time seem to decrease with increasing molecule size, though the savings in all three cases are very similar. For the HRPA(D) model the savings for the medium sized molecule seems largest and as expected from Figure 12a, there is a large variation in the time savings for the different molecules.

This large variation of time reduction might be investigated further by considering also the number of iterations necessary for the zeroth-order problems (i.e., RPA and HRPA) to be solved as well as the absolute SOPPA calculation time. This is shown in Figure 13.

Clearly, when the iteration count is increased the general trend in Figure 13a is that the reduction in calculation time is

lowered for HRPA(D), while it remains almost constant for RPA(D). This indicates that the main difference in the calculation time of the two models is caused by the need to solve the larger HRPA problem, which includes the second-order contributions to the **A** and **B** matrices, in the case of HRPA(D).

From Figure 13b it can be seen that as the number of iterations required for the HRPA(D) (and hence HRPA) model approaches the number of iterations required for a SOPPA calculation, the reduction in calculation time is decreased as anticipated in section "Computational cost of doubles corrected methods." Actually, it appears that three different trends can be seen for HRPA(D); one trend shows a large time reduction (calculations taking 30%–40% of a SOPPA calculation) almost independent of the savings in iterations, another showing calculation times of 60%–80% of the SOPPA time and only some dependency on the iteration reduction, and finally a trend is shown for a dramatic dependency of the time reduction on the iteration count compared to SOPPA. The time reduction given by the RPA(D) model, however, seems unaffected by the required number of iterations compared to those needed for the SOPPA calculation.

Figure 13c shows the calculation time in percentage of SOPPA calculation time vs. the absolute SOPPA calculation time, which scales with the size of the molecule considered. For short SOPPA calculation times the computationally cheaper models are of less interest, and so the trends for the longer lasting calculations over 120 min is of greatest interest here. Also, the shorter calculations are expected to be more affected by other calculations running simultaneously. It is observed for the longer running calculations shown in Figure 13c that, while the time reduction of RPA(D) is almost constant with increasing SOPPA calculation time, the HRPA(D) model shows an almost linear increase in calculation time. As only few molecules are considered here, this should be investigated further as this conclusion might not apply for all systems. However, the results here seem already to indicate that the time savings offered by

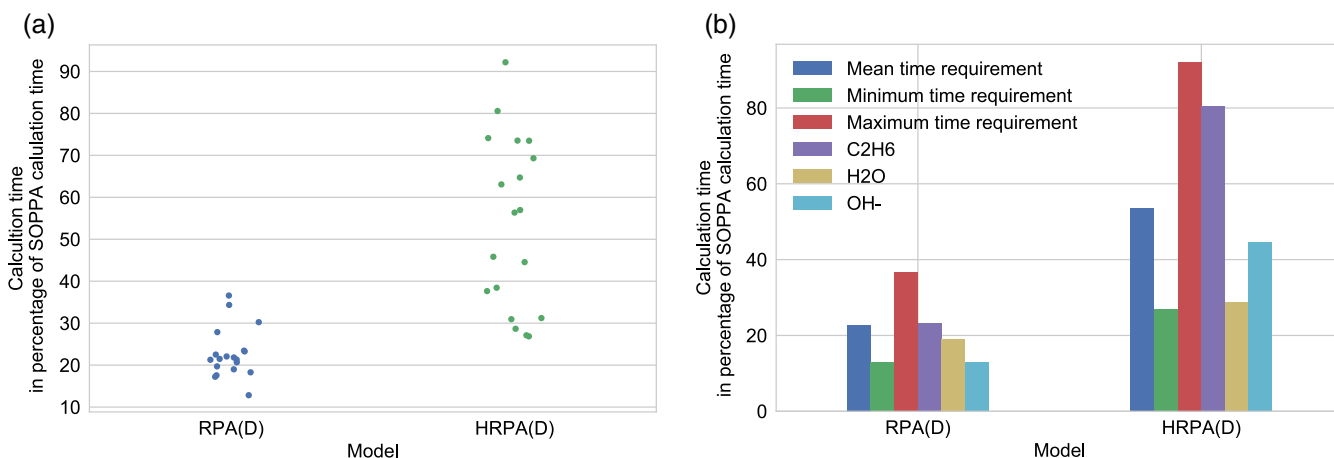


Figure 12. Calculation time of the two doubles corrected models in percentage of SOPPA calculation CPU time for the investigated molecules. Calculation times for a small (OH^-) medium sized (H_2O) and larger (C_2H_6) molecule has been shown explicitly on the right. NF_3 has not been included as convergence for the SOPPA model for this molecule could not be obtained under the same conditions as for the doubles corrected models. [Color figure can be viewed at www.onlinelibrary.com]

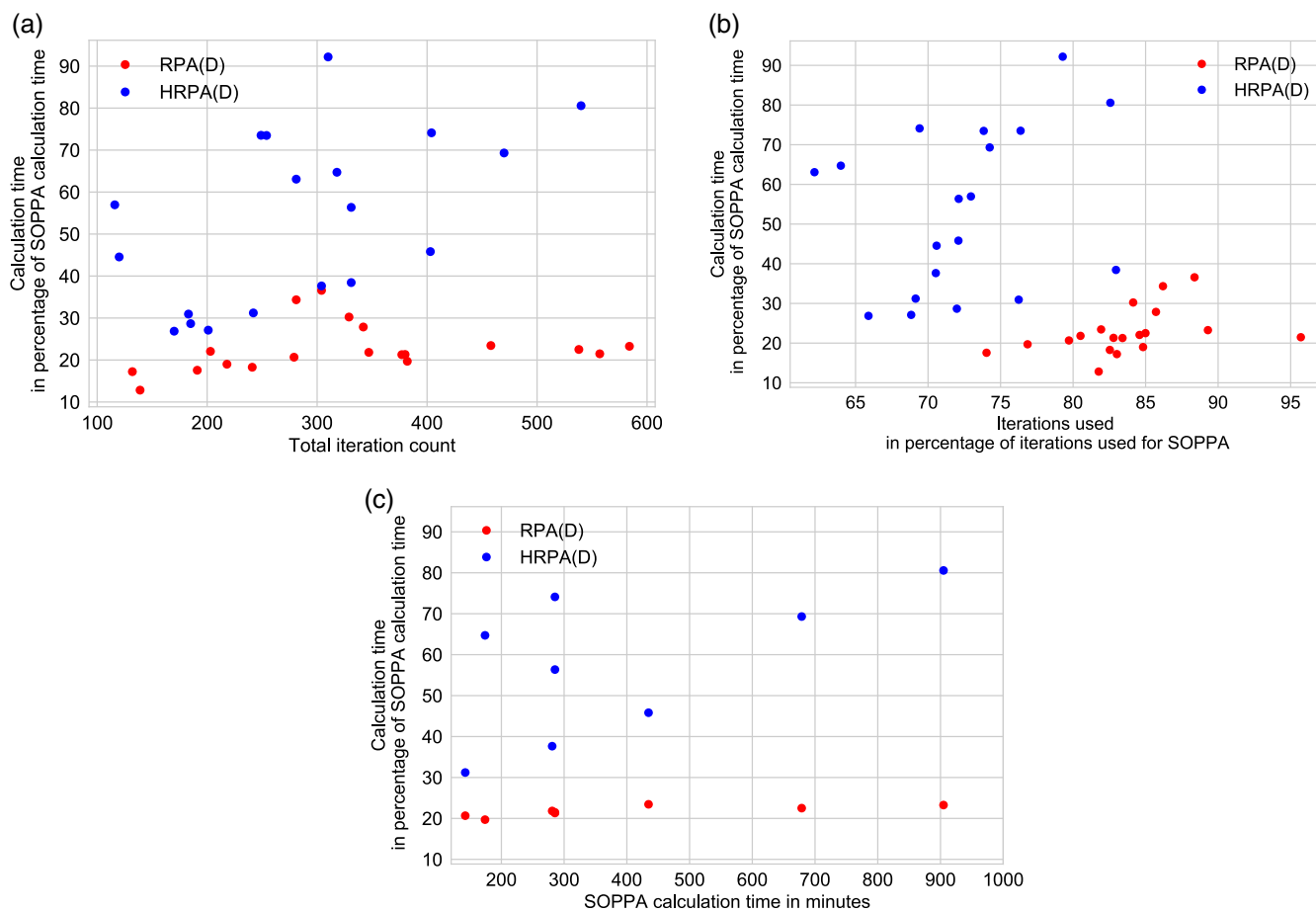


Figure 13. The calculation time in percentage of SOPPA calculation time versus (a) the total number of iterations required for a calculation with the given model, (b) the fraction of iterations required compared to the number required for SOPPA, and (c) the absolute SOPPA calculation time. (a) Calculation time versus iteration count for the doubles corrected models. (b) Calculation time of the doubles corrected models versus iteration fraction. (c) Calculation time of the doubles corrected models versus SOPPA calculation time from 120 min to 1000 min. [Color figure can be viewed at wileyonlinelibrary.com]

HRPA(D) even for larger molecules will be less significant than those offered by the RPA(D) model.

Thus, while the HRPA(D) model may yield results of higher accuracy than RPA(D) compared to the CCSD model, the time saved is difficult to predict and can be quite small. The RPA(D) model on the other hand generally yields a large reduction in calculation time as well as results of good accuracy compared to the CCSD model.

Concluding Remarks

The RPA(D) and HRPA(D) models for linear response properties have been derived and successfully implemented in the DALTON program, and both seem to offer a substantial improvement on the RPA and HRPA models, respectively, for the properties investigated in this study. For the coupling types investigated here the HRPA(D) model was shown to be comparable in accuracy to the SOPPA model, but the time reduction was not impressive. The RPA(D) model on the other hand was shown to reduce the calculation time substantially for all molecules as well as yielding results of good accuracy, although it might have issues with triplet instabilities, which is not seen for

HRPA(D). While the RPA(D) results were not of quite as high accuracy compared to the CCSD model as the HRPA(D) model, the time reduction more than makes up for that. Hence, the RPA(D) model is recommended as a cheap alternative to the SOPPA model for large molecules.

Bearing in mind the small test set, further investigations of the trends observed here should be carried out on a larger benchmark set without couplings to fluorine, as both the RPA and HRPA models, as well as the doubles corrected models, were observed to have trouble describing couplings of this type.

For a better idea of the overall quality of the models, investigations of model performance could also be carried out using a more accurate model than the CCSD model as a reference.

Furthermore, studies of model performance on different types of nuclear spin–spin coupling constants as well as different properties should be carried out for all models, as the encouraging results obtained for the indirect nuclear spin–spin coupling constants and its contributions in this study might not be representative of the overall performance of the new models.

Finally, it should be noted that the efficiency of the calculations could be further improved for all models if the resolution


of identity approximation was used, or other techniques for atomic integral calculations were implemented.

Acknowledgments

FFP acknowledges financial support from CONICET and UNNE (PI: 15/F002 Res. 1017/15 C.S). SPAS thanks the Danish Center for Scientific Computing (DCSC) and the TWAS Visiting Expert Programme (F.R. 3240301376) for financial support.

Keywords: SOPPA · RPA(D) · HRP(A) · linear response properties · indirect nuclear spin–spin coupling constant

How to cite this article: A. K. Schnack-Petersen, P. A. B. Haase, R. Faber, P. Provasi, S. P. A. Sauer. *J. Comput. Chem.* **2018**, *39*, 2647–2666. DOI: 10.1002/jcc.25712

 Additional Supporting Information may be found in the online version of this article.

- [1] T. Helgaker, M. Jaszuński, K. Ruud, *Chem. Rev.* **1999**, *99*, 293.
- [2] T. Helgaker, M. Jaszuński, M. Pecul, *Prog. Nucl. Magn. Reson. Spectrosc.* **2008**, *53*, 249.
- [3] L. B. Krivdin, *Prog. Nucl. Magn. Reson. Spectrosc.* **2018**, *105*, 54.
- [4] L. B. Krivdin, S. V. Zinchenko, *Curr. Org. Chem.* **1998**, *2*, 173.
- [5] R. H. Contreras, J. E. Peralta, *Prog. NMR Spectrosc.* **2000**, *37*, 321.
- [6] J. I. Olsen, S. P. A. Sauer, C. M. Pedersen, M. Bols, *Org. Biomol. Chem.* **2015**, *13*, 3116.
- [7] A. Bagno, F. Rastrelli, G. Saielli, *Prog. Nucl. Magn. Reson. Spectrosc.* **2005**, *47*, 41.
- [8] J. C. Hierso, *Chem. Rev.* **2014**, *114*, 4838.
- [9] G. I. Pagola, M. B. Ferraro, S. Pelloni, P. Lazzeretti, S. P. A. Sauer, *Theor. Chem. Accounts* **2011**, *129*, 359.
- [10] H. Kjaer, M. R. Nielsen, G. I. Pagola, M. B. Ferraro, P. Lazzeretti, S. P. A. Sauer, *J. Comput. Chem.* **2012**, *33*, 1845.
- [11] A. A. Auer, J. Gauss, *J. Chem. Phys.* **2001**, *115*, 1619.
- [12] A. A. Auer, J. Gauss, *J. Chem. Phys.* **2009**, *356*, 7.
- [13] A. A. Auer, J. Gauss, M. Pecul, *Chem. Phys. Lett.* **2003**, *368*, 172.
- [14] R. Faber, S. P. A. Sauer, J. T. Gauss, *J. Chem. Theory Comput.* **2017**, *13*, 696.
- [15] H. Sekino, R. J. Bartlett, *J. Chem. Phys.* **1986**, *85*, 3945.
- [16] S. A. Perera, H. Sekino, R. J. Bartlett, *J. Chem. Phys.* **1994**, *101*, 2186.
- [17] S. A. Perera, M. Nooijen, R. J. Bartlett, *J. Chem. Phys.* **1996**, *104*, 3290.
- [18] M. Nooijen, S. A. Perera, R. J. Bartlett, *Chem. Phys. Lett.* **1997**, *266*, 456.
- [19] A. Perera, *Mol. Phys.* **2010**, *108*, 3017.
- [20] J. Geertsens, J. Oddershede, *Chem. Phys.* **1984**, *90*, 301.
- [21] T. Enevoldsen, J. Oddershede, S. P. A. Sauer, *Theor. Chem. Accounts* **1998**, *100*, 275.
- [22] H. Kjaer, S. P. A. Sauer, J. Kongsted, *J. Chem. Phys.* **2010**, *133*, 144106.
- [23] T. Helgaker, S. Coriani, P. Jørgensen, K. Kristensen, J. Olsen, K. Ruud, *Chem. Rev.* **2012**, *112*, 543.
- [24] D. Bohm, D. Pines, *Phys. Rev.* **1951**, *82*, 625.
- [25] D. J. Rowe, *Rev. Mod. Phys.* **1968**, *40*, 153.
- [26] P. F. Provasi, G. A. Aucar, S. P. A. Sauer, *J. Chem. Phys.* **2001**, *115*, 1324.
- [27] D. P. Tew, W. Klopper, T. Helgaker, *J. Comput. Chem.* **2007**, *28*, 1307.
- [28] O. B. Lutnæs, T. Helgaker, M. Jaszuński, *Mol. Phys.* **2010**, *108*, 2579.
- [29] T. Kupka, M. Nieradka, M. Stachow, T. Pluta, P. Nowak, H. Kjaer, J. Kongsted, J. Kaminsky, *J. Phys. Chem. A* **2012**, *116*, 3728.
- [30] T. Shibuya, V. McKoy, *J. Chem. Phys.* **1970**, *53*, 3308.
- [31] M. Head-Gordon, R. J. Rico, M. Oumi, T. J. Lee, *Chem. Phys. Lett.* **1994**, *219*, 21.
- [32] M. Head-Gordon, D. Maurice, M. Oumi, *Chem. Phys. Lett.* **1995**, *246*, 114.
- [33] M. Head-Gordon, M. Oumi, D. Maurice, *Mol. Phys.* **1999**, *96*, 593.
- [34] O. Christiansen, K. L. Bak, H. Koch, S. P. A. Sauer, *Chem. Phys. Lett.* **1998**, *284*, 47.
- [35] P. A. B. Haase, R. Faber, P. F. Provasi, S. P. A. Sauer. To be submitted
- [36] P.-O. Åstrand, P. S. Ramanujam, S. Hvilsted, K. L. Bak, S. P. A. Sauer, *J. Am. Chem. Soc.* **2000**, *122*, 3482.
- [37] P.-O. Åstrand, P. Sommer-Larsen, S. Hvilsted, P. S. Ramanujam, K. L. Bak, S. P. A. Sauer, *Chem. Phys. Lett.* **2000**, *325*, 115.
- [38] H. H. Falden, K. R. Falster-Hansen, K. L. Bak, S. Rettrup, S. P. A. Sauer, *J. Phys. Chem. A* **2009**, *113*, 11995.
- [39] S. P. A. Sauer, H. F. Pitzner-Frydendahl, M. Buse, H. J. A. Jensen, W. Thiel, *Mol. Phys.* **2015**, *113*, 2026.
- [40] O. Christiansen, H. Koch, P. Jørgensen, *J. Chem. Phys.* **1996**, *105*, 1451.
- [41] N. F. Ramsey, *Phys. Rev.* **1953**, *91*, 303.
- [42] S. P. A. Sauer, *Molecular Electromagnetism*, Oxford University Press, Oxford, **2011**.
- [43] S. P. A. Sauer, *J. Chem. Phys.* **1993**, *98*, 9220.
- [44] P. Lazzeretti, *J. Chem. Phys.* **2012**, *137*, 74108.
- [45] E. Nielsen, P. Jørgensen, J. Oddershede, *J. Chem. Phys.* **1980**, *73*, 6238.
- [46] J. Olsen, P. Jørgensen, T. Helgaker, J. Oddershede, *J. Phys. Chem. A* **2005**, *109*, 11618.
- [47] M. Packer, E. K. Dalskov, T. Enevoldsen, H. J. Jensen, J. Oddershede, *J. Chem. Phys.* **1996**, *105*, 5886.
- [48] K. L. Bak, H. Koch, J. Oddershede, O. Christiansen, S. P. A. Sauer, *J. Chem. Phys.* **2000**, *112*, 4173.
- [49] K. Aidas, C. Angeli, K. L. Bak, V. Bakken, R. Bast, L. Boman, O. Christiansen, R. Cimraglia, S. Coriani, P. Dahle, E. K. Dalskov, U. Ekström, T. Enevoldsen, J. J. Eriksen, P. Ettenhuber, B. Fernández, L. Ferrighi, H. Fiegler, L. Frediani, K. Hald, A. Halkier, C. Hättig, H. Heiberg, T. Helgaker, A. C. Hennum, H. Hettema, E. Hjertenæs, S. Høst, I. Høyvik, M. F. Iozzi, B. Jansík, H. J. A. Jensen, D. Jonsson, P. Jørgensen, J. Kauczor, S. Kirpekar, T. Kjærgaard, W. Klopper, S. Knecht, R. Kobayashi, H. Koch, J. Kongsted, A. Krapp, K. Kristensen, A. Ligabue, O. B. Lutnæs, J. I. Melo, K. V. Mikkelsen, R. H. Myhre, C. Neiss, C. B. Nielsen, P. Norman, K. O. Sylvester-Hvid, P. R. Taylor, A. M. Teale, E. I. Tellgren, D. P. Tew, A. J. Thorvaldsen, L. Thøgersen, O. Vahtras, M. A. Watson, D. J. D. Wilson, M. Ziolkowski, H. Ågren, *WIREs Comput. Mol. Sci.* **2014**, *4*, 269.
- [50] U. Benedikt, A. A. Auer, F. Jensen, *J. Chem. Phys.* **2008**, *129*, 4111.
- [51] R. Faber, S. P. A. Sauer, *Theor. Chem. Accounts* **2018**, *137*, 1.
- [52] J. Oddershede, *Adv. Quantum Chem.* **1978**, *11*, 275.
- [53] S. Berger, S. Braun, H. O. Kalinowski, *Carbon-13 NMR Spectroscopy*, Wiley, Chichester, **1988**.
- [54] D. Moy, A. R. Young, *J. Am. Chem. Soc.* **1965**, *87*, 1889.
- [55] S. Berger, S. Braun, H. O. Kalinowski, *NMR Spectroscopy of the Non-Metallic Elements*, Wiley, New York, **1997**.
- [56] I. Alkorta, P. F. Provasi, G. A. Aucar, J. Elguero, *Magn. Reson. Chem.* **2008**, *46*, 356.
- [57] Faber, R.; Kaminsky, J.; Sauer, S. P. A. *Gas Phase NMR*; Jackowski, K., Jaszuński, M., Royal Society of Chemistry, London. **2016**, ch. 7, p 218.
- [58] R. D. Wigglesworth, W. T. Raynes, S. Kirpekar, J. Oddershede, S. P. A. Sauer, *J. Chem. Phys.* **2000**, *112*, 3735.
- [59] R. D. Wigglesworth, W. T. Raynes, S. Kirpekar, J. Oddershede, S. P. A. Sauer, *J. Chem. Phys.* **2001**, *114*, 9192.
- [60] A. Yachmenev, S. N. Yurchenko, I. Paidarová, P. Jensen, W. Thiel, S. P. A. Sauer, *J. Chem. Phys.* **2010**, *132*, 114, 305.
- [61] R. Faber, S. P. A. Sauer, *Phys. Chem. Chem. Phys.* **2012**, *14*, 16,440.
- [62] R. Faber, S. P. A. Sauer, *AIPL Conf. Proc.* **1702**, 2015, 90,035.
- [63] A. Møgelhøj, K. Aidas, K. V. Mikkelsen, S. P. A. Sauer, J. Kongsted, *J. Chem. Phys.* **2009**, *130*, 508.
- [64] K. Ruud, L. Fredani, R. Cammi, B. Mennucci, *Int. J. Mol. Sci.* **2003**, *4*, 119.

Received: 21 June 2018

Revised: 26 August 2018

Accepted: 23 September 2018

Published online on 23 November 2018